nature communications

Article

https://doi.org/10.1038/s41467-024-51144-9

# Restriction of arginine induces antibiotic tolerance in *Staphylococcus aureus*

Received: 14 November 2023

Accepted: 31 July 2024

Published online: 07 August 2024

Check for updates

Jeffrey A. Freiberg[1,2] ✉, Valeria M. Reyes Ruiz[2,3], Brittney D. Gimza[4], Caitlin C. Murdoch[2,3], Erin R. Green[2,3,5], Jacob M. Curry[4], James E. Cassat[2,3,4,6,7] & Eric P. Skaar[2,3] ✉

*Staphylococcus aureus* is responsible for a substantial number of invasive infections globally each year. These infections are problematic because they are frequently recalcitrant to antibiotic treatment. Antibiotic tolerance, the ability of bacteria to persist despite normally lethal doses of antibiotics, contributes to antibiotic treatment failure in *S. aureus* infections. To understand how antibiotic tolerance is induced, *S. aureus* biofilms exposed to multiple anti-staphylococcal antibiotics are examined using both quantitative proteomics and transposon sequencing. These screens indicate that arginine metabolism is involved in antibiotic tolerance within a biofilm and support the hypothesis that depletion of arginine within *S. aureus* communities can induce antibiotic tolerance. Consistent with this hypothesis, inactivation of *argH*, the final gene in the arginine synthesis pathway, induces antibiotic tolerance. Arginine restriction induces antibiotic tolerance via inhibition of protein synthesis. In murine skin and bone infection models, an *argH* mutant has enhanced ability to survive antibiotic treatment with vancomycin, highlighting the relationship between arginine metabolism and antibiotic tolerance during *S. aureus* infection. Uncovering this link between arginine metabolism and antibiotic tolerance has the potential to open new therapeutic avenues targeting previously recalcitrant *S. aureus* infections.

*S taphylococcus aureus* is one of the leading bacterial causes of mortality in the world[1], with mortality rates in excess of 20% for certain types of infections[2–9]. These high mortality rates are due, in part, to high rates of antibiotic treatment failure that occur during the treatment of *S. aureus* infections. Anti-staphylococcal penicillins or first-generation cephalosporins are first-line treatment options for *S. aureus* infections. Although Methicillin-resistant *S. aureus* (MRSA) strains with resistance to these first-line agents are relatively common, the rates of multi-drug resistance to anti-MRSA antibiotics remains very low[10,11]. In this context, the high rates of antibiotic treatment failure are surprising and suggest a mechanism besides antibiotic resistance. Multiple studies have investigated potential causes of antibiotic treatment failure in *S. aureus* and have identified a variety of contributory factors including the formation of small colony variants (SCVs), persister cells, and biofilms[12–19].

Growth as a biofilm, a dense community where adherent microbes secrete a complex extracellular matrix, induces extremely high levels of antibiotic tolerance. Antibiotic tolerance is the ability of a bacterial

[1]Division of Infectious Diseases, Department of Medicine, Vanderbilt University Medical Center, Nashville, TN, USA. [2]Vanderbilt Institute for Infection, Immunology and Inflammation, Vanderbilt University Medical Center, Nashville, TN, USA. [3]Department of Pathology, Microbiology and Immunology, Vanderbilt University Medical Center, Nashville, TN, USA. [4]Division of Pediatric Infectious Diseases, Department of Pediatrics, Vanderbilt University Medical Center, Nashville, TN, USA. [5]Department of Microbiology, University of Chicago, Chicago, IL, USA. [6]Vanderbilt Center for Bone Biology, Vanderbilt University Medical Center, Nashville, TN, USA. [7]Department of Biomedical Engineering, Vanderbilt University, Nashville, TN, USA. ✉e-mail: jeffrey.freiberg@vumc.org; eric.skaar@vumc.org

population to withstand an otherwise lethal antibiotic dose due to phenotypic changes without any evidence of a change in the minimum inhibitory concentration (MIC) against that antibiotic[20]. Bacteria growing in a biofilm community differ from planktonic bacteria in their metabolism and growth, and they are able to tolerate 100 to 1000 times the concentration of antibiotics that would eliminate planktonic bacteria[21]. Biofilm formation has been implicated in many different types of *S. aureus* infections including osteomyelitis, prosthetic joint infections, endocarditis, and chronic wound infections[22]. In these infections, biofilm growth contributes to the high morbidity and recalcitrance to antibiotic treatment.

Despite much investigation and speculation about the potential causes of antibiotic tolerance in biofilm-mediated infections, the mechanisms by which this occurs in *S. aureus* are still poorly understood. In this work, an in vitro model of *S. aureus* biofilms grown at a solid-air interface is employed to investigate antibiotic tolerance during biofilm growth. Mechanisms of antibiotic tolerance in *S. aureus* are identified using two broad, unbiased, complementary screening approaches: semi-quantitative proteomics, and transposon sequencing-based screening. These screens identify a novel role for arginine metabolism as a key potentiator of antibiotic tolerance in *S. aureus*. By restricting the synthesis of arginine, *S. aureus* can induce antibiotic tolerance by inhibition of protein synthesis. Furthermore, inhibiting the ability of *S. aureus* to produce arginine from citrulline during antibiotic treatment enhances bacterial fitness during antibiotic treatment in mouse models of skin and soft tissue infection (SSTI) and osteomyelitis. Together, these studies demonstrate that restricting arginine synthesis, and in turn limiting arginine availability, can contribute to antibiotic treatment failure in *S. aureus*.

## Results

### Antibiotic exposure results in differences in protein abundance and relative fitness of transposon mutants in arginine metabolism pathways in *S. aureus*

To screen for proteins that are involved in antibiotic tolerance in *S. aureus* biofilms, untargeted, label-free, quantitative (LFQ) proteomics using liquid chromatography tandem mass spectrometry (LC-MS/MS) was performed. For LFQ proteomic analysis, *S. aureus* JE2, a derivative of the MRSA USA300 LAC strain, was grown in a colony filter biofilm model. *S. aureus* biofilms formed in this model have a matrix consisting of a mixture of bacteria, extracellular DNA (eDNA), polysaccharides, and protein (Figure S1). This model allows for the establishment of a mature biofilm at a solid-air interface which can be easily transferred to different growth conditions while keeping the biofilm structure intact[23]. This provides a useful in vitro model of the type of biofilm that might form in a wound infection, of which *S. aureus* is a frequent cause[24–27]. Utilizing this model, *S. aureus* biofilms grown on polycarbonate filter discs on tryptic soy agar (TSA) plates could be transferred as intact biofilms to fresh media every 24 h (Figure S2a). After 48 h of growth in antibiotic-free conditions, mature biofilms were transferred to TSA plates containing antibiotics for an additional 48 h. To identify pathways that are involved in tolerance to multiple antibiotics, four different classes of antibiotics were used: vancomycin, a cell wall targeting glycopeptide and the most commonly used first line antibiotic for the treatment of MRSA bacteremia worldwide[28]; ceftaroline, a cell wall targeting beta-lactam antibiotic with activity against MRSA; linezolid, an oxazolidinone that inhibits protein synthesis and has activity against MRSA; and delafloxacin, a fourth generation fluoroquinolone with activity against MRSA. Antibiotic concentrations were 400 μg/ml for vancomycin, 20 μg/ml for ceftaroline, 20 μg/ml for linezolid, and 9 μg/ml for delafloxacin. These concentrations, with the except of vancomycin, were chosen based on published peak serum concentrations for standard clinical treatment doses[29], and represent concentrations >200x, >20x, 10x, and >40x the MICs, respectively. Bacterial killing resulting from antibiotic treatment of these biofilms after 24 and 48 h is shown in Figure S2b. After 48 h of exposure to antibiotics or a no-antibiotic control, total protein was extracted from the colony biofilms and identified using LC-MS/MS. Based on this analysis, there were a total of 142 proteins with significant differences in their abundance when treated with one of the antibiotics tested (Supplementary Data 1).

As a complementary approach to performing LFQ proteomics, a transposon library was constructed in the JE2 strain using a Himar1-based transposon approach as previously described in ref. 30. This resulted in the creation of a high quality, high-density transposon library with greater than 150,000 independent transposon insertions representing coverage of nearly 55% of all TA sites and at least one TA site in 93.3% of annotated open reading frames in the USA300_FPR3757 genome (2619 out of 2807) (Figure S3). Analysis of the library using the TRANSIT software package[31] revealed 369 essential genes in the *S. aureus* genome, in line with estimates from other studies in *S. aureus*[32,33]. Another 227 genes were labeled as uncertain as their small size limited the ability to confidently predict their essentiality. To screen for genes impacting survival in the presence of antibiotics, the transposon library was grown using the colony filter biofilm model and exposed to antibiotics for 48 h, as above. Following antibiotic treatment, a 4 h outgrowth in tryptic soy broth (TSB) as a planktonic culture was performed to enrich the population of viable bacteria. Following the outgrowth, DNA was extracted, and transposon sequencing was performed. Based on analysis of the sequencing results using TRANSIT, 157 genes were either essential or detrimental to survival in at least one of the antibiotic conditions tested (Supplementary Data 2). In addition to identifying genes important for survival in the presence of antibiotics, this experiment also identified genes that significantly impacted fitness during biofilm growth (Supplementary Data 3).

Analysis of the datasets resulting from the LFQ proteomics and TnSeq experiments revealed that very few protein-gene pairs were identified by both techniques. However, transposon insertions disrupting either of two genes encoded in an operon, *argG* and *argH*, were found to be beneficial for survival in the presence of multiple antibiotics and the corresponding encoded proteins were decreased in abundance in response to treatment with all the antibiotics tested (Fig. 1). Together, ArgG and ArgH are responsible for the synthesis of L-arginine from L-citrulline (Fig. 1a). Evaluation of several other enzymes involved in arginine metabolism, ArgD, ArgC, ArgJ, ArgB, and RocD, did not show any significant differences in the proteomic or TnSeq datasets. However, the enzymes responsible for degrading arginine via the arginine deiminase pathway, ArcA, ArcB, and ArcC, showed increased abundance during exposure to 3 out of the 4 antibiotics tested for both the operon located on the native chromosomal DNA and on the Arginine Catabolism Mobile Element (ACME) genomic island (Fig. 1b). Transposon insertions in *arcA, arcB*, and *arcC* did not lead to any significant fitness differences (Fig. 1c). Together, these results suggest a coordinated metabolic response leading to increased arginine degradation and decreased arginine synthesis occurs in response to antibiotics during biofilm growth.

### Arginine is required for growth and limited within a *S. aureus* biofilm

Since arginine metabolism was implicated as having a role in antibiotic tolerance in both screens, we sought to better understand the role of arginine within *S. aureus* biofilms. *S. aureus* is unique in that it contains intact copies of the genes encoding all of the enzymes necessary to synthesize arginine from glutamate or proline, but is auxotrophic for arginine during planktonic growth[34–38]. Given its requirement for arginine during planktonic growth, we hypothesized that exogenous arginine was also required for growth in a biofilm. Consistent with the phenotype reported for planktonic growth, JE2 was unable to grow when inoculated as a biofilm on chemically defined media lacking arginine (CDM-R) (Fig. 2a). Likewise, when a 48-hour old colony filter

https://doi.org/10.1038/s41467-024-51144-9

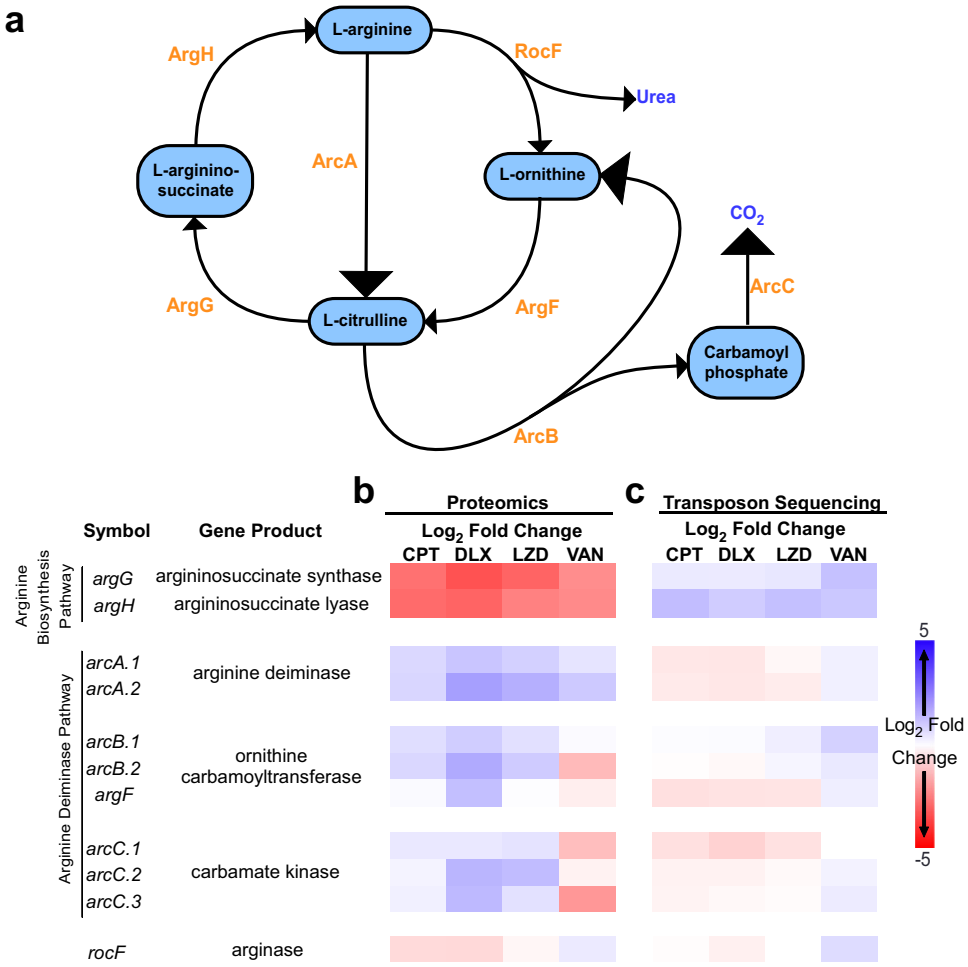


**Fig. 1 | Arginine metabolism in *S. aureus* biofilms during antibiotic exposure.** **a** Diagram showing the flux of arginine in *S. aureus*, which involves the urea cycle and the arginine deiminase pathway. The responsible enzymes for each step are shown in orange. **b** Mature (48 h) *S. aureus* (strain JE2) colony biofilms grown on polycarbonate filters placed on TSA plates were transferred to fresh TSA plates either with vehicle or with one of the indicated antibiotics added. Total protein was isolated after 48 h of exposure to the antibiotic containing media, and relative protein abundance was determined by label free quantitative LC-MS/MS proteomics. The heat map shows the *z*-scores of the $\log_2$ fold difference in the abundance of the indicated proteins involved in arginine metabolism after antibiotic exposure compared to the no antibiotic control. **c** A transposon mutant library was constructed in the JE2 background and used to grow colony biofilms. The colony biofilms were transferred to TSA plates with or without antibiotics for 48 h after which point the biofilms were harvested and after a short outgrowth in TSB total genomic DNA was extracted for transposon sequencing. Heat map shows the *z*-scores of the $\log_2$ fold difference in the normalized read counts for transposon insertions in the indicated genes involved in arginine metabolism after antibiotic exposure compared to the no antibiotic control. The notation *arcA.1*, *arcB.1*, and *arcC.1* refer to the genes located on the chromosomal arginine deiminase operon while *arcA.2*, *arcB.2*, and *arcC.2* refer to the genes located in the arginine deiminase operon found on the ACME. All experiments were done in biological triplicates. VAN vancomycin, CPT ceftaroline, DEL delafloxacin, LZD linezolid.

biofilm was transferred to CDM-R, it not only was unable to grow, but it had decreased survival (Fig. 2b). To determine the availability of amino acids in *S. aureus* biofilms, amino acids were extracted from 48-hour old colony filter biofilms and sent to the VUMC Analytic Services Core for analysis. Amino acid analysis of biofilms grown on both TSA and CDM (containing arginine) revealed that, even when arginine is present in the growth media, the level of free arginine in the biofilm is undetectable (Fig. 2c). Collectively, this suggests that exogenous arginine is essential for growth in *S. aureus*. Furthermore, its availability is likely one of the growth-limiting factors within a biofilm, since all other essential amino acids for which *S. aureus* is auxotrophic were detected in at least one of the two media conditions (Fig. 2c).

## Restriction of arginine induces antibiotic tolerance

To understand whether arginine availability influences antibiotic tolerance, *S. aureus* was grown as colony filter biofilms on CDM for 48 h and then the intact biofilms were transferred to either CDM or CDM-R with or without antibiotics added (Fig. 3a, c, e, g). When arginine was present in the media, all four of the antibiotics led to least a 1-log reduction in CFUs by 72 h, when compared to the starting CFU. This was a significant reduction when compared to the untreated biofilms for all four of the antibiotics. When biofilms were transferred to media without arginine, there was a decrease in CFUs even in the absence of antibiotics. However, the addition of antibiotics to the media without arginine did not cause any further decrease in the number of CFUs when compared to the untreated biofilms, suggesting there was no effect from antibiotic treatment under arginine-restricted conditions. The only exception to this was delafloxacin, where only after 72 h of antibiotic exposure in the absence of arginine was there a significant decrease in CFUs compared to the untreated biofilms (Fig. 3e). However, this reduction in CFUs was still less than the reduction seen in biofilms treated with delafloxacin in the presence of arginine.

To determine if the effect of arginine on antibiotic tolerance was specific to growth in a biofilm, *S. aureus* was grown planktonically in shaking liquid culture, harvested during its logarithmic growth phase, washed, and transferred to either CDM or CDM-R with antibiotics

https://doi.org/10.1038/s41467-024-51144-9

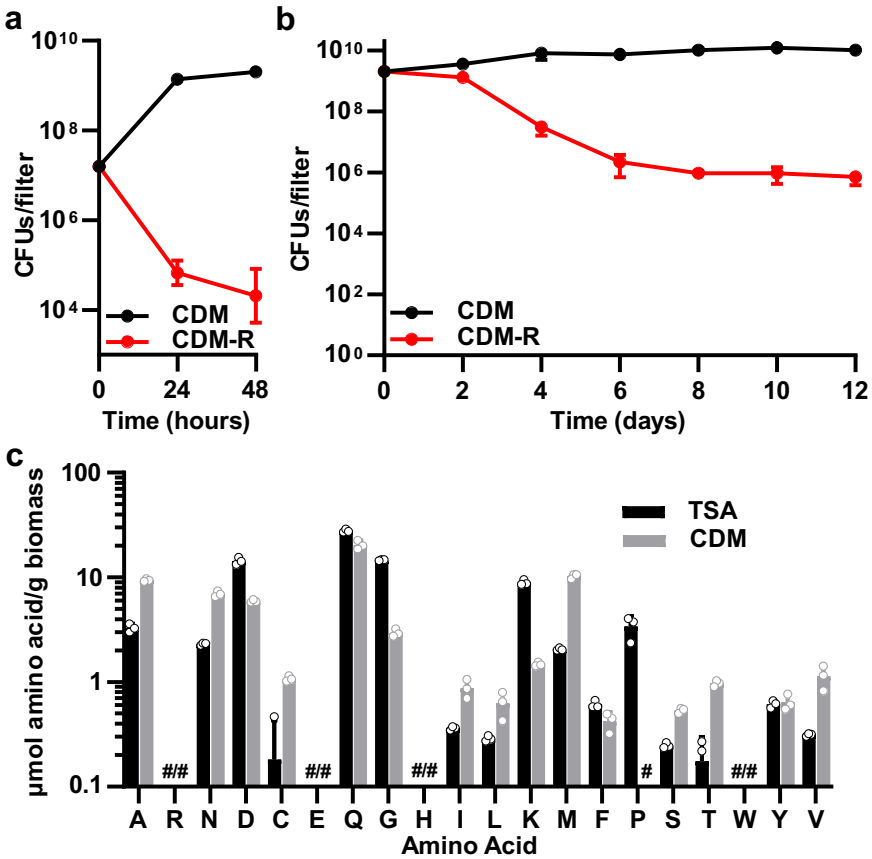


**Fig. 2 | Arginine is important for growth and survival in *S. aureus* biofilms. a** JE2 is unable to establish colony biofilms when inoculated on filters on chemically defined media (CDM) in the absence of arginine, and (**b**) mature (48 h) biofilms grown on chemically defined media with arginine present have reduced survival when transferred to media lacking arginine (CDM-R). **c** Arginine levels are below the limit of detection in *S. aureus* biofilms grown on either TSA or CDM agar plates. # = below the limit of detection. **a**–**c** Data represent technical replicates of biological triplicates, mean ± SD shown. Source data are provided as a Source Data file.

(Fig. S4). In planktonic culture, the absence of arginine only induced substantial antibiotic tolerance against ceftaroline (Fig. S4b). By contrast, vancomycin, delafloxacin, and linezolid all showed greater than 2-log reductions in the number of CFUs after 48 h of antibiotic exposure, even in the absence of arginine. Despite this, the presence of arginine in planktonic cultures did lead to a significant increase in killing by vancomycin. Differences in susceptibility to delafloxacin, however, varied over time with significantly more killing in the absence of arginine by 48 h.

Since high concentrations of arginine weaken the integrity of biofilms in some bacterial species[39], we hypothesized that the observed effect of arginine might be due to changes in the extracellular matrix or increased antibiotic penetration within the biofilm[39]. To test this hypothesis, 48 h colony filter biofilms were homogenized, washed with PBS, and resuspended in either CDM or CDM-R broth. The homogenized biofilms were then exposed to antibiotics. Mechanically disrupted biofilms exhibited greater susceptibility to antibiotics overall when compared to intact biofilms. However, in the disrupted biofilms there was an even more pronounced difference in the amount of antibiotic killing based on the presence or absence of arginine (Fig. 3b, d, f, h). For vancomycin, ceftaroline, and delafloxacin there was significantly more antibiotic tolerance when arginine was absent. After 48 h of antibiotic exposure, for these three antibiotics there was a greater than 100-fold difference in the number of CFUs between cultures with and without arginine. This increase in antibiotic tolerance in the absence of arginine was not restricted to JE2, as a similar increase in tolerance to vancomycin was seen with both the laboratory MSSA strain Newman and a clinical MRSA isolate (Figure S5). Arginine restriction showed a dose-response effect as tolerance to vancomycin increased as the starting arginine concentration of the media decreased (Fig. S6a). Homogenized biofilm bacteria deplete arginine from the extracellular media over 24 h, but depletion of arginine is not seen in the presence of vancomycin, suggesting that, in the presence of high levels of arginine, bacteria are not able to deplete arginine fast enough to overcome the bactericidal effects of the antibiotic (Fig. S6b). In homogenized JE2 biofilms, however, there was no difference in bacterial killing between the cultures with and without arginine when they were treated with linezolid, with both conditions having less than a single log reduction in CFUs. These experiments suggest an effect of arginine on antibiotic susceptibility that is dependent on the metabolism of *S. aureus* during biofilm growth, but independent of the biofilm structure.

### Restriction of arginine increases antibiotic tolerance through the inhibition of protein synthesis

The finding that, as opposed to the three other antibiotics, *S. aureus* biofilms display high levels of tolerance to linezolid regardless of arginine concentrations was intriguing. This led us to hypothesize that a pathway affected by both arginine depletion and linezolid might be responsible for the induction of antibiotic tolerance. Since linezolid is a protein synthesis inhibitor, inhibition of protein synthesis was hypothesized to be a shared pathway to induce tolerance. Although linezolid is classified as a bacteriostatic antibiotic, the concentration used in this study was sufficient to cause over a 2-log reduction in CFUs in planktonic cultures in either TSB or CDM (Figs. S2, S4). To confirm that restriction of arginine leads to inhibition of protein synthesis, nascent

https://doi.org/10.1038/s41467-024-51144-9

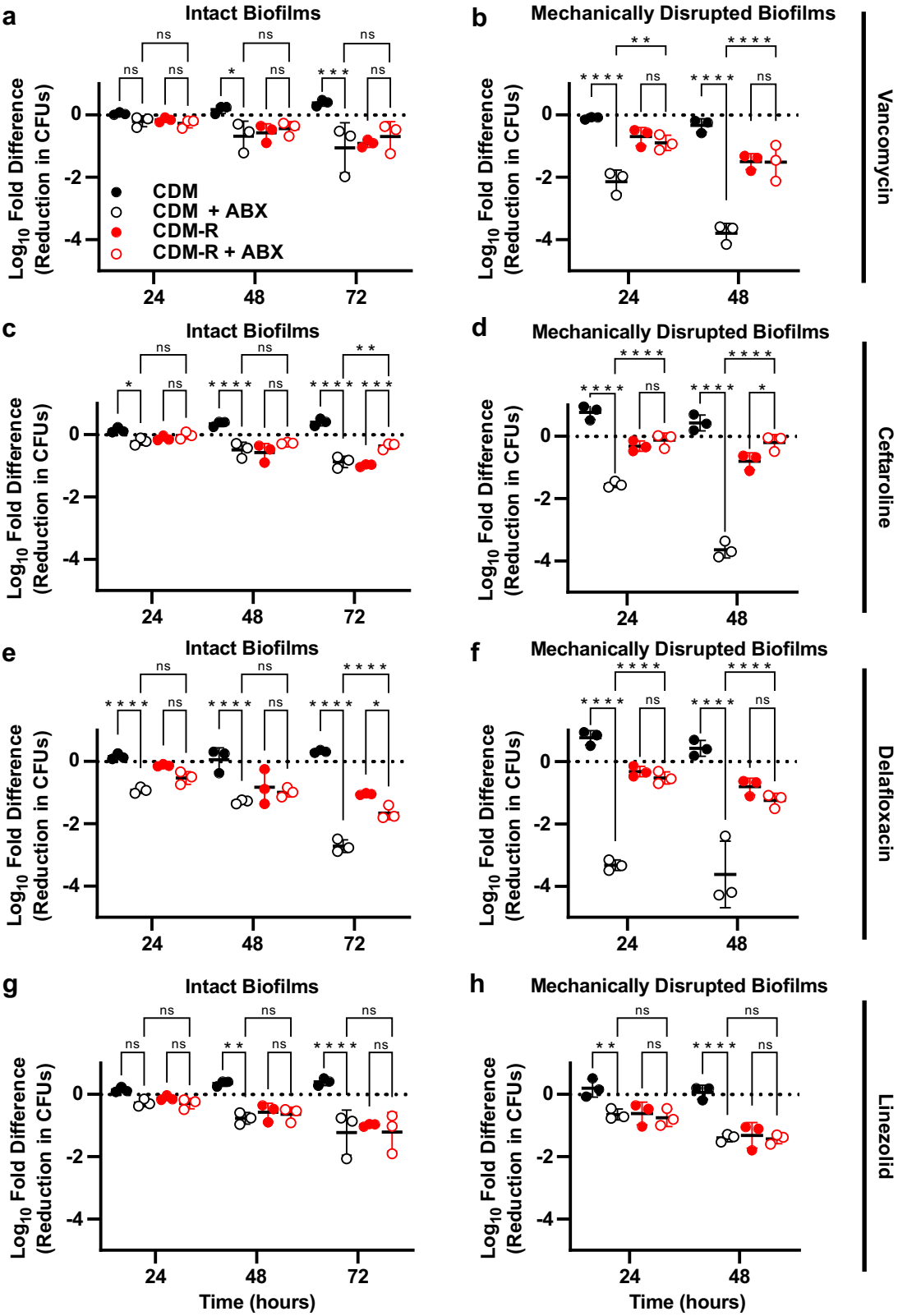


**Fig. 3 | Arginine deprivation induces tolerance to multiple classes of antibiotics in *S. aureus biofilms*.** Colony biofilms grown for 48 h on polycarbonate filters on CDM agar plates were either transferred to fresh CDM or CDM-R plates with or without antibiotics (**a**, **c**, **e**, **g**) or were homogenized and transferred to liquid CDM or CDM-R media with or without antibiotics added (**b**, **d**, **f**, **h**) The following concentration of antibiotics were used: 400 μg/ml vancomycin (**a**, **b**), 20 μg/ml ceftaroline (**c**, **d**), 9 μg/ml delafloxacin (**e**, **f**), and 20 μg/ml linezolid (**g**, **h**). **a**–**h** Data represent technical replicates of biological triplicates, mean ± SD shown. 2-way ANOVA with Tukey multiple comparisons test; * = $p < 0.05$, ** = $p < 0.005$, *** = $p < 0.0005$, **** = $p < 0.0001$, ns not significant, ABX antibiotics. Source data are provided as a Source Data file.

protein labeling was performed using click chemistry. Biofilms grown for 48 h on CDM agar were homogenized and transferred to CDM broth lacking arginine in which L-methionine had been replaced with the methionine analog L-homopropargylglycine (L-HPG). After 4 h bacteria were harvested, and nascent proteins were labeled to allow for visualization and quantification via western blot (Fig. 4a). Normalization of the integrated density of the fluorescence signal for each sample by the total protein (Fig. S7) confirmed that there was significant inhibition of protein synthesis in the absence of arginine (Fig. 4b). Furthermore, the addition of citrulline reversed this inhibition of protein synthesis, presumably due to the conversion of citrulline to arginine via the ArgGH enzymes.

To validate that inhibition of protein synthesis is the mechanism by which arginine depletion leads to antibiotic tolerance, two other experiments were performed. The first experiment tested whether the depletion of other amino acids for which *S. aureus* is known to display auxotrophy also induces antibiotic tolerance. Similar to what was observed in media without arginine present, the removal of either valine or proline, two essential amino acids that *S. aureus* is unable to normally synthesize[34], increased the tolerance of *S. aureus* biofilms to vancomycin, ceftaroline, and delafloxacin (Fig. 4c). By contrast, removal of the non-essential amino acid alanine had no impact on antibiotic tolerance. Notably, proline and valine could be detected in biofilms grown in TSA, albeit at low levels (Fig. 2c), suggesting that these amino acids are not restricted to the degree that arginine is within *S. aureus* biofilms. Consistent with this hypothesis, transposon insertions in the genes in the proline or valine biosynthetic pathways (*proC, rocD, ilvA-E*) did not show significant impacts on fitness in the presence of antibiotics in TSA (Supplementary Data 2).

As a secondary experiment to validate that protein synthesis inhibition leads to antibiotic tolerance, the ability of multiple protein synthesis inhibitors to induce antibiotic tolerance was tested. Biofilms grown for 48 h on CDM agar were homogenized and transferred to liquid media either lacking a protein synthesis inhibitor or containing one of three protein synthesis inhibitors (linezolid, doxycycline, or clindamycin). The addition of any one of these antibiotics that inhibit protein synthesis resulted in increased tolerance to ceftaroline, similar to what was seen in media lacking arginine (Fig. 4d). Together, these experiments suggest inhibition of protein synthesis through multiple pathways, including the depletion of arginine, induces antibiotic tolerance in *S. aureus* biofilms.

Finally, to confirm that arginine-depletion dependent inhibition of protein synthesis still occurred in the presence of antibiotics, the nascent protein labeling experiments were repeated as above, but also with the addition of vancomycin both in the presence and absence of arginine. Similar to what was observed in the absence of antibiotics, there is arrest of protein synthesis when arginine is restricted in the presence of vancomycin, but there is ongoing protein synthesis when arginine is present, even if vancomycin is added (Fig. 4e, Fig. S8).

### Antibiotic tolerance mediated by arginine-deprivation is dependent on the stringent response

Inhibition of protein synthesis from amino acid starvation is known to induce the stringent response in *S. aureus*[40]. Since activation of the stringent response can induce tolerance to antibiotics, we hypothesized that this mechanism likely explained some, if not the majority, of the means by which arginine depletion ultimately leads to antibiotic tolerance[41]. To test this hypothesis, we utilized a *S. aureus* strain, *relA*::Tn, which contains a transposon mutation in the C-terminal domain of the RelA bifunctional (p)ppGpp synthetase/hydrolase[33]. Disruption of the C-terminal domain of RelA preserves the hydrolase function of RelA, which is essential, but disrupts its normal synthetase function by preventing interaction with the bacterial ribosome[42]. Consistent with a role for the stringent response in arginine-deprivation mediated antibiotic tolerance, the presence or absence of arginine in the media did not affect the susceptibility to vancomycin in the *relA*::Tn mutant (Fig. 4f). An arginine dependent effect on tolerance was subsequently restored by complementation of *relA* under its native promoter.

### ArgGH-mediated conversion of citrulline to arginine can reverse arginine-deprivation mediated antibiotic tolerance and contributes to antibiotic susceptibility in vivo

Since the addition of citrulline to CDM broth lacking arginine could restore protein synthesis, it was next hypothesized that the addition of citrulline could reverse the antibiotic tolerance observed when arginine was depleted. When grown in planktonic culture, citrulline rescued the growth of JE2 in media lacking arginine but could not do so for *argH*::Tn, a strain of JE2 in which the *argH* gene was disrupted by a transposon insertion (Figure S9). As expected, the addition of citrulline reversed the antibiotic tolerance seen when arginine was absent from the media (Fig. 5a). This effect was most likely due to the conversion of citrulline to arginine as citrulline did not restore antibiotic susceptibility when the experiment was repeated using *argH*::Tn (Fig. 5b). Furthermore, when the *argGH* operon was reintroduced into the chromosome of the *argH*::Tn strain under a constitutively active promoter, *S. aureus* was once again able to utilize citrulline for growth (Figure S9) and also showed increased antibiotic susceptibility in the presence of citrulline (Fig. 5c).

Chronically infected wounds have been shown to have elevated levels of citrulline, presumably due to metabolism of arginine by the host immune system[43]. Since disruption of *argH* resulted in the inability of *S. aureus* to convert citrulline into arginine and a subsequent increase in antibiotic tolerance in vitro, it was hypothesized that ArgH might play an important role in antibiotic susceptibility during treatment of a *S. aureus* wound infection. Using a murine model of a skin and soft tissue infection (SSTI)[44], the ability of the *argH*::Tn strain to survive antibiotic treatment was compared directly to that of the parental strain, JE2. A patch of skin was exposed on the back of mice by tape-stripping, and the exposed epidermis was then inoculated with a mixture of both the JE2 and *argH*::Tn strains at a 2:1 WT:mutant ratio. Murine *S. aureus* SSTI models, including this tape-stripping model, promote *S. aureus* infections with local biofilm formation[45–48]. The SSTI was allowed to progress for 48 h, at which point mice received either antibiotic treatment with IP injections of vancomycin or a vehicle control. After 48 hours of treatment, mice were euthanized, and individual lesions were excised to quantify the number of CFUs of each strain present. As a control, a subset of mice was harvested at 48 hours post-inoculation (prior to any antibiotic treatment) to determine relative fitness of the two strains in the absence of antibiotics. As shown in Figure S10, there were large differences in the response to a *S. aureus* skin infection between male and female mice, with female mice showing a significant reduction in the number of total CFUs even in the absence of antibiotic treatment, consistent with sex differences previously shown in *S. aureus* mouse skin infections[49]. However, the changes within the ratio of mutant to wildtype (as measured by a competitive index), were relatively consistent across both sexes. Concentrations of arginine and citrulline present in the mouse skin were similar between the two sexes, and on a similar order of magnitude to the concentrations used in the in vitro experiments (Figure S11). Among all mice (male and female combined), in the absence of antibiotic treatment, there was a significant decrease in fitness of the *argH*::Tn mutant relative to the parental control at both 2 DPI and 4 DPI (one-sample Wilcoxon test, $p = 0.0066$ and $p < 0.0001$, respectively) (Fig. 5d), in line with previous studies showing a virulence defect in an *argH* mutant during infection[35]. A similar phenotype was observed when the male and female mice were analyzed individually (Figure S10). Conversely, the *argH* mutant had a higher competitive index in the vancomycin treatment group when compared to either the pretreatment or vehicle control treated groups (Fig. 5d), consistent

https://doi.org/10.1038/s41467-024-51144-9

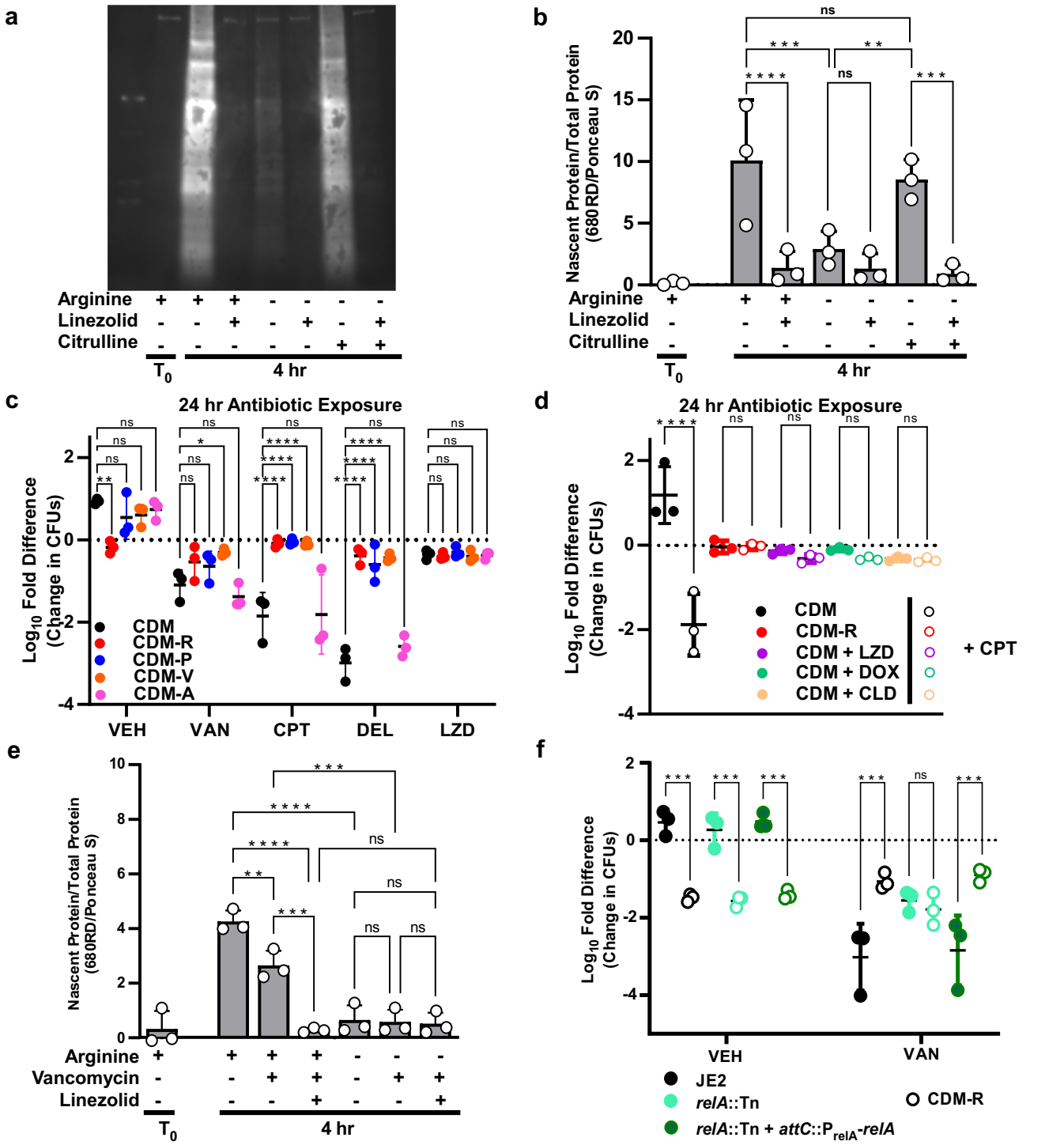


**Fig. 4 | Antibiotic tolerance is mediated by amino acid starvation leading to protein synthesis arrest. a** Representative western blot showing the labelling of nascent protein by click chemistry 4 h after the transfer of homogenized biofilm cultures to the indicated growth conditions. The first lane contains Bio-Rad Precision Plus Protein Ladder with 50 kDa band visible. See figure S7 for corresponding full ladder. **b** A ratio of nascent protein to total protein was calculated using integrated density values obtained by analyzing the western blots in imageJ. Data represent biological triplicates, mean ± SD shown. 2-way ANOVA with Tukey multiple comparisons test. **c** Homogenized biofilm cultures were transferred to CDM broth or CDM broth lacking individual amino acids and antibiotics were added as indicated. The reduction in CFUs compared to the starting inoculum was calculated after 24 h of antibiotic exposure. **d** Homogenized biofilm cultures were transferred to fresh CDM or CDM-R and protein synthesis inhibitors were added as indicated along with either ceftaroline or a vehicle control. The reduction in CFUs compared to the starting inoculum was calculated after 24 h of antibiotic exposure. **e** The ratio of nascent protein to total protein in the presence or absence of vancomycin was calculated from integrated density values obtained by analysis of biological triplicates of western blots in imageJ. Data represent biological triplicates, mean ± SD shown. 1-way ANOVA with Tukey multiple comparisons test. **f** Arginine depletion does not affect antibiotic tolerance in a *relA*::Tn mutant even after 48 h of antibiotic exposure. **c**, **d**, **f** Data represent technical replicates of biological triplicates, mean ± SD shown. 2-way ANOVA with Tukey multiple comparisons test; *=$p < 0.05$, **=$p < 0.005$, ***=$p < 0.0005$, ****=$p < 0.0001$, ns not significant, VEH no antibiotic vehicle control, VAN vancomycin, CPT ceftaroline, DEL delafloxacin, LZD linezolid, DOX doxycycline, CLD clindamycin. Source data are provided as a Source Data file.

https://doi.org/10.1038/s41467-024-51144-9

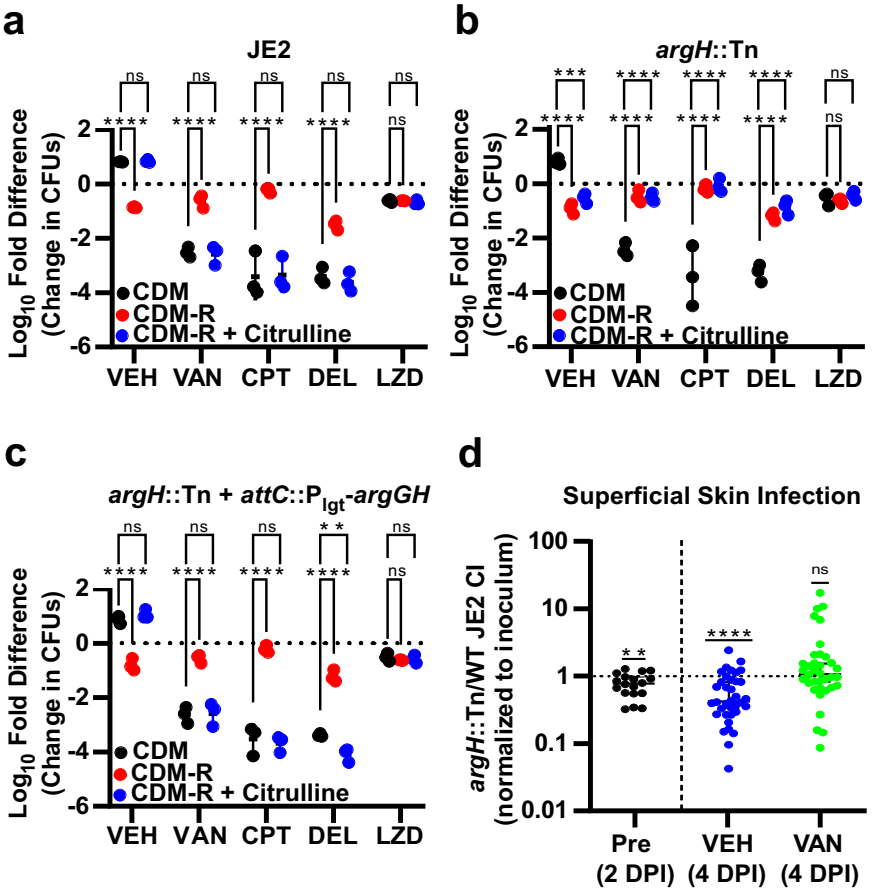


**Fig. 5 | Presence of citrulline restores antibiotic susceptibility in an ArgH dependent manner. a** Addition of citrulline to CDM-R restores the antibiotic susceptibility of homogenized colony biofilms to CDM levels. **b** Antibiotic susceptibility is not restored by the addition of citrulline in an *argH*::Tn mutant. **c** complementation with the *argGH* operon in the *argH*::Tn mutant restores antibiotic susceptibility to wild-type levels in the presence of citrulline. Data represent technical replicates of biological triplicates. **d** Competitive index (CI) for *argH*::Tn/JE2 competition experiment in a murine superficial skin infection model. Data shown are the ratio of *argH*::Tn to JE2 CFUs, normalized to the ratio of the starting inoculum, at 2 days post infection (DPI) prior to any treatment along with the ratio after 48 h of vancomycin or vehicle control treatment (4 DPI). Data represent the combined results from a total of 90 mice (45 females and 45 males). Two-sided Wilcoxon Signed Rank Test, median with 95% CI shown. **a**–**c** Data represent technical replicates of biological triplicates, mean ± SD shown. 2-way ANOVA with Tukey multiple comparisons test. *=$p < 0.05$, **=$p < 0.005$, ***=$p < 0.0005$, ****=$p < 0.0001$, ns not significant, VEH no antibiotic vehicle control, VAN vancomycin, CPT ceftaroline, DEL delafloxacin, LZD linezolid. Source data are provided as a Source Data file.

with the hypothesis that lower levels of ArgH are beneficial to *S. aureus* during antibiotic treatment. These experiments support a role for the conversion of citrulline into arginine by ArgGH in influencing antibiotic tolerance during an infection.

To further confirm the role of ArgH in antibiotic tolerance during biofilm-mediated infections, a murine osteomyelitis model with vancomycin treatment was also employed[50]. Biofilms play an important role in osteomyelitis and contribute to the high rates of antibiotic treatment failure seen in the treatment of this type of infection[13]. In this model, mice were inoculated directly in their femurs with JE2 and *argH*::Tn at a 2:1 WT:mutant ratio and treated with vancomycin for seven days beginning immediately at the time of infection. Consistent with the recalcitrance of osteomyelitis to vancomycin treatment, 7 out of the 10 mice treated with vancomycin remained infected after 7 days of antibiotic treatment, despite starting therapy immediately (Figure S12a). Similar to what was observed in the SSTI model, the *argH*::Tn mutant had decreased fitness in the absence of antibiotics, but had a relative advantage during treatment with vancomycin (Figure S12b).

## Discussion

Through the experiments detailed above, we uncovered a previously unappreciated relationship between arginine availability, arginine metabolism, protein synthesis, and antibiotic tolerance in *S. aureus*. This relationship was elucidated with the help of two broad screening approaches carried out in parallel, LFQ proteomics and TnSeq. With the exception of the enzymes involved in arginine metabolism, there were very few gene/protein pairs identified as hits in both datasets, however both techniques provide important insight and complementary information. Both screens independently identified different sets of genes that have been previously shown to influence antibiotic susceptibility[51–57]. As an example, the proteomics approach is useful for identifying changes in protein abundance that may be missed through a transposon screen due to functional redundancy or compensatory mechanisms. This likely explains why components of the arginine deiminase pathway were identified in the proteomics screen, but not in the transposon screen. Conversely, our transposon screen can identify effects related to lower abundance proteins that cannot be accurately quantified via LFQ proteomics or proteins whose functions are controlled by post-translational regulation or other mechanisms that do not involve changes in total abundance to exert their influence. This is the case for many genes identified as contributing to antibiotic tolerance in our transposon screen (*graXRS, arlRS, mprF*, and *vraFG*, among others) that did not show significant differences or were not found in the proteomic dataset, but are already known to influence antibiotic susceptibility in *S. aureus* during planktonic growth[54–57].

Our experimental design also allowed us to identify genes that were required for biofilm growth (Supplementary Data 3). However, since genes required for survival in a biofilm were selected against by the 48 h of biofilm growth that occurred prior to antibiotic exposure, we were unable to test their contribution to antibiotic tolerance directly. It is likely that many of these genes that contribute to biofilm fitness also play a role in antibiotic tolerance and may warrant further investigation. As an example, VraSR, the vancomycin-resistance-associated two component system is known to be associated with susceptibility to vancomycin[51] and the proteomics experiments showed significant increases in levels of VraS, VraR, and the majority of the proteins known to make up the VraSR regulon (Supplementary Data 1)[58]. However, *vraR* and *vraS* mutants were found to be essential for biofilm growth (Supplementary Data 3), and therefore not identified as having decreased fitness in the presence of vancomycin in our transposon screen. This highlights one of the benefits of our complementary screening approach. A similar explanation may explain why genes such as *ychF, ndh2, spsA, addA, purE, bfmBAB*, and *sgtB*, all of which were increased in abundance in the proteomic screen and essential for biofilm growth in our transposon screen, were not identified as playing a role in fitness during antibiotic exposure in our transposon sequencing experiment.

While an unanticipated finding from our screen, a connection between antibiotic tolerance and arginine metabolism is not entirely unprecedented. Studies in other bacterial species have found that arginine and arginine metabolism can impact antibiotic susceptibility, including during biofilm growth[59–63]. Although arginine can disrupt the extracellular matrix of bacterial biofilms at very high concentrations[39], arginine's primary effect on antibiotic tolerance in *S. aureus* is not through disruption of the biofilm. To exclude the possibility that arginine affects antibiotic susceptibility by disrupting extracellular matrix, biofilms were homogenized for the majority of the experiments in this work. In these experiments, biofilm bacteria were resuspended in shaking liquid cultures at a high concentration to preserve the high density, nutrient-limited conditions found in a biofilm. This technique also effectively removed any antibiotic tolerance that was the result of variable penetration of an antibiotic within a biofilm from our experiments. Not only was a difference between media with and without arginine preserved under these conditions, but the difference in antibiotic susceptibility was enhanced for all the antibiotics tested. This is in contrast to the relatively minor effect of arginine deprivation on susceptibility in planktonic cultures (Figure S4). Presumably, this is because bacteria within the *S. aureus* biofilm already exist within a low arginine state (Fig. 2). Although removal of arginine from the media does increase antibiotic tolerance (Fig. 3), the biofilm, on the whole, is likely more polarized to an arginine deprived state, which explains the high baseline level of antibiotic tolerance.

The ability of linezolid and other antibiotics that inhibit protein synthesis to induce antibiotic tolerance similar to what was seen in arginine depletion (Fig. 4d), supports inhibition of protein synthesis as a common mechanism. This is consistent with other work showing that bacteriostatic, protein synthesis inhibiting antibiotics can antagonize the action of bactericidal antibiotics including cell wall targeting antibiotics[64]. Furthermore, inhibition of protein synthesis from amino acid starvation triggers the stringent response in *S. aureus* which induces tolerance to antibiotics[40,41]. The results presented in this study (Fig. 4f) suggest that the stringent response is the major mechanism by which arginine-deprivation mediated antibiotic tolerance occurs.

There has been a growing appreciation for the role of antibiotic tolerance in *S. aureus* treatment failure which has coincided with the uncovering of multiple mechanisms by which tolerance is induced. Depletion of ATP, inhibition of the TCA cycle by reactive oxygen species (ROS), and induction of the stringent response have all been tied to antibiotic tolerance in *S. aureus*[65–68]. It is not yet clear where arginine depletion fits within these other mechanisms. However, it is intriguing that arginine has direct ties to these other pathways, as not only is arginine deprivation likely to induce the stringent response through amino acid starvation but arginine can be used as an alternative source of ATP production[69]. Furthermore, arginine is essential for the production of the ROS nitric oxide by host macrophages[70], suggesting that production of ROS by the host immune system may be tied directly to the depletion of arginine during an infection. While outside the scope of these studies, it would be interesting to investigate the connection between arginine depletion and tolerance specifically within the context of interaction with host immune cells.

The ability of *S. aureus* to induce tolerance by restricting its own arginine synthesis pathway may explain a long-standing paradox-namely that wildtype *S. aureus* has fully functional arginine synthesis enzymes yet does not synthesize arginine under any in vitro conditions that have been tested thus far[36,37]. In line with other studies, *S. aureus* was unable to grow without arginine (Fig. 2). Among the enzymes in the arginine synthesis pathway, only ArgG and ArgH were found at levels above the limit of detection in our proteomic dataset. ArgD, ArgC, ArgJ, and ArgB were not found, consistent with other work showing these enzymes are under high levels of transcriptional repression[35–37,71].

The detection of differences in the levels of the ArgG and ArgH proteins in response to antibiotic treatment is particularly interesting in the context of the existing paradigm of regulation of this operon. The *argGH* operon is transcriptionally repressed under glucose replete conditions by CcpA and transcriptionally repressed under arginine replete conditions by AhrC[37]. Mutations in these repressors allow for the transcription of the *argGH* operon and the subsequent growth of *S. aureus* in the absence of arginine through the utilization of proline[35], However, the absence of both glucose and arginine is not sufficient to overcome this repression in a wildtype background, suggesting there is also glucose independent repression due to CcpA[36,37]. Arginine and glucose both quickly become limited within the biofilm in the colony filter biofilm model, which explains why expression of ArgG and ArgH was observed. Although citrulline was able to rescue growth in the absence of arginine in an ArgH dependent manner (Figure S9), the presence of proline in the media was not sufficient to restore growth in the absence of arginine within a biofilm (Fig. 2a, b), consistent with the current understanding that proline is not an adequate source for arginine biosynthesis due to glucose-independent repression of *putA* by CcpA[36]. Given this regulation pattern, it is unclear by what mechanism antibiotics would lead to lower levels of ArgG and ArgH within a biofilm as their transcription should remain de-repressed by the low glucose, low arginine environment. Another recently identified regulator of *argGH* is the small RNA *teg58*[72]. However, *teg58* is repressed by SarA[72], and SarA expression is induced by vancomycin[73], making *teg58* unlikely to be responsible for the decreased levels of the ArgG and ArgH proteins that are observed. It appears there is some yet unrecognized mechanism responsible for the decreased abundance of these enzymes, and it warrants further investigation as it may elucidate a further understanding of how *S. aureus* responds to antibiotics within a biofilm.

*S. aureus* contains multiple enzymatic pathways that catabolize arginine, which helps create an environment that can rapidly consume any exogenous arginine, thus limiting the availability of arginine for protein synthesis. These pathways likely maintain a low baseline level of arginine in *S. aureus* biofilms, as evidenced by the inability to detect arginine within mature biofilms (Fig. 2c). The isolate used in this study, JE2, is a representative USA300 strain, which has become the most common *S. aureus* strain type in the United States[74]. Intriguingly, almost all USA300 strains have two full copies of the arginine deiminase pathway due to a second copy that is contained within the ACME[75]. The acquisition of the ACME has been postulated to be related to the success of USA300 strains, although the mechanisms underlying

this connection have not been completely delineated. This second arginine deiminase pathway may be contributing to the success of USA300 through a role in antibiotic tolerance, a hypothesis furthered by the fact that the ACME arginine deiminase pathway is constitutively expressed as opposed to the native arginine deiminase pathway that is only expressed under anaerobic conditions[76]. While there was some variability across the proteomic dataset in the levels of the arginine deiminase pathway enzymes based on the antibiotic tested, increases in the abundance of both copies of ArcA, the first enzyme in the pathway, were seen across all four antibiotics tested (Fig. 1).

Although *S. aureus* was unable to synthesize arginine in the presence of glutamate or proline (Fig. 2), it was able to utilize exogenous citrulline to synthesize arginine presumptively via ArgG and ArgH activity (Fig. S9). The ability of exogenous citrulline to increase antibiotic susceptibility was shown in this study both in vitro (Fig. 5a, b, and c) and in vivo in infection and treatment models as part of a competition experiment (Fig. 5d, S12). In this model, an *argH* mutant had a relative fitness defect compared to the parental JE2 strain, consistent with a prior in vivo study using the *argH* mutant[35]. However, disruption of *argH* led to an increase in the relative fitness of the mutant during vancomycin treatment. Together, these studies support the idea that the conversion of citrulline to arginine through ArgH is an important source of arginine for *S. aureus*. Plasma arginine and citrulline levels are decreased in humans during sepsis[77,78], suggesting a possible opportunity for a therapeutic intervention that improves antibiotic effectiveness by increasing levels of amino acids at the site of an infection. The uncovering of this previously underexplored connection between bacterial metabolism, arginine availability, and antibiotic tolerance represents an exciting new target to help overcome antibiotic treatment failure.

## Methods

### Ethics statement

This research complies with all relevant ethical regulations. All mouse studies were approved by the VUMC Institutional Animal Care and Use Committee.

### Bacterial strains and growth conditions

JE2 is a previously described strain derived from the MRSA USA300 LAC[33]. Newman is a previously described MSSA strain[79]. *S. aureus* CI 5296 is a clinical *S. aureus* isolate that was obtained from the VUMC clinical microbiology laboratory with approval from the VUMC Institutional Review Board. CI 5296 was initially isolated from the blood culture of a patient with endocarditis. Antibiotic susceptibility testing initially performed as part of routine clinical microbiology laboratory testing identified CI 5296 as methicillin-resistant, with susceptibility to ceftaroline (MIC 0.5), linezolid (MIC ≤ 1), and vancomycin (MIC = 2). Strain *argH*::Tn was constructed by phage transduction of a*rgH*::*erm* from the Nebraska Transposon Mutant Library (NTML) strain NE106 into JE2 via φ85. Strain *relA*::Tn was constructed by phage transduction of *relA*::*erm* from the NTML strain NE1714 into JE2 via φ85. The *argH*::Tn complemented strain, *argH*::Tn + *attC*::$P_{lgt}$-*argGH*, was constructed using the pJC1111 vector for chromosomal integration at the SaPI1 attachment site as previously described in ref. 80. Briefly, *argGH* was cloned into pOS1 downstream of the *lgt* promoter using primers 5′-aa tacaattgaggtgaacatatgaaagagaaaattgttttag-3′ and 5′-cccttgtttggatcctc gagttattgtgatagtaattgtttagc-3′ to PCR the *argGH* operon and primers 5′-ctcgaggatccaaacaag-3′ and 5′-atgttcacctcaattgtatttatc-3′ to linearize pOS1. The resulting PCR fragments were assembled using NEBuilder HiFi DNA Assembly (New England Biolabs, Rowley, MA). The plasmid product from this assembly was used as a template to clone $P_{lgt}$-*argGH* by PCR with primers 5′-ctgcaggtcgactctagaggactaatgatttattatgta gtggttc-3′ and 5′-taggcgcgcctgaattcgagttattgtgatagtaattgtttagc-3′. The pJC1111 vector was linearized using the primers 5′- ctcgaattcaggc gcgcctattct-3′ and 5′-cctctagagtcgacctgcaggcatg-3′ and then pJC1111-$P_{lgt}$-*argGH* was assembled using NEBuilder HiFi DNA Assembly. The resulting plasmid was transformed into RN4220/pRN7023 and once chromosomal integration was confirmed the constructed was transferred into the JE2 a*rgH*::*erm* background by phage transduction of via φ85. $P_{relA}$-*relA* was amplified from genomic JE2 DNA using the primers 5′-ctgcaggtcgactctagaggaataatataatttttatcaaatg aaatccttc-3′ and 5′-taggcgcgcctgaattcgagctagttccaaactcttgttac-3′ and cloned into linearized pJC1111 before ultimately being transduced into the JE2 *relA*::*erm* background. Correct construction of these strains was confirmed by PCR as previously described for the NTML[33] and by whole genome sequencing (SeqCoast Genomics).

*S. aureus* was routinely grown in planktonic culture in Tryptic Soy Broth (TSB; Becton, Dickinson and Company) at 37 °C with shaking at 180 rpm when not explicitly grown as a biofilm. When indicated, antibiotics were added to growth media to the following concentrations- 400 μg/ml vancomycin (Fresenius Kabi), 20 μg/ml ceftaroline (Sigma Aldrich), 9 μg/ml delafloxacin (Sigma Aldrich), 20 μg/ml linezolid (Thermo Scientific Chemicals), 2.1 μg/ml doxycycline (Sigma Aldrich), and 14 μg/ml clindamycin (Thermo Scientific Chemicals). With the exception of vancomycin antibiotic concentrations used were chosen based on the peak serum concentrations for standard clinical treatment doses as published in the Sanford Guide to Antimicrobial Therapy[29]. Chemically defined medium (CDM) was prepared as described in ref. 81. with the correction that the concentration of magnesium sulfate heptahydrate in the stock salt solution was 2.56 g/L (instead of 25.6 g/L). When indicated, CDM was prepared with the omission of individual amino acids. CDM agar was prepared by combining the necessary stock salt solution, amino acids, and bases with 15 g/L agarose and autoclaving the media prior to the addition of the vitamin solution, trace elements, and any antibiotics as indicated.

### Colony filter biofilm assay

Colony biofilms were grown on membrane filters in a manner similar to Anderl et al. [23]. Overnight cultures of *S. aureus* were pelleted by centrifugation, washed with phosphate buffered saline (PBS), and diluted to an OD600 of 0.1. Polycarbonate membrane filters (13-mm diameter; 0.2 μm pore size) (Whatman) were placed on top of nutrient agar plates and were inoculated by placing 10 μl of the diluted overnight culture on the center of the filter. The agar plates containing the filters were incubated upside down at 37 °C, and filters were transferred to fresh nutrient agar plates every 24 h. Biofilms were homogenized by placing filters in 1.5 mL Navy Eppendorf Bead Lysis Kits (Next Advance, Inc) with 1 mL PBS and homogenizing them using a Bullet Blender Tissue Homogenizer (Next Advance, Inc) run for 3 successive cycles of 4 minutes at max speed at 4 °C. Serial dilutions of the homogenates were plated to determine CFUs. For antibiotic susceptibility testing of intact biofilms, filters containing mature (48 h old) biofilms were transferred to fresh nutrient agar plates containing the indicated antibiotics. Filters were transferred to fresh antibiotic containing nutrient agar plates every 24 h until they were homogenized and CFUs were determined by plating serial dilutions. Each experiment was repeated in triplicate with technical replicates used each time. Data were analyzed using either Student T-test or 2-way ANOVA depending on the number of conditions being tested, with the appropriate corrections for multiple comparisons included.

### Planktonic antibiotic susceptibility testing

To test the antibiotic susceptibility of planktonic JE2, overnight cultures were diluted 1:100 into prewarmed TSB and grown at 37 °C, shaking at 180 rpm. After 2 h of growth (mid-exponential phase), cultures were removed from the incubator, pelleted by centrifugation, washed with PBS, and diluted to an OD600 of 0.5 in fresh TSB. This culture was split into individual aliquots and antibiotics were added to the final concentrations outlined above. These cultures were returned to the 37 °C shaking incubator for the remainder of the experiment. At

4, 24, and 48 h, 1 mL aliquots of each culture were removed, pelleted by centrifugation, washed with PBS, and resuspended in 1 mL before being plated to determine CFUs by serial plating. In the case of experiments examining the role of arginine on planktonic antibiotic susceptibility, a similar procedure was employed with the exception that the overnight culture of JE2 was diluted 1:100 into CDM instead of TSB. For these experiments, after washing the mid-exponential cultures with PBS, the cells were resuspended in CDM without arginine. This culture was then split into two aliquots, and L-arginine (Sigma Aldrich) was added to one aliquot to a final concentration of 400 μM L-arginine (the concentration of arginine in CDM) before the cultures were split further and antibiotics were added.

### Proteomic sampling

Mature colony filter biofilms inoculated and grown on TSA as above were transferred to TSA plates either without antibiotics or with vancomycin, ceftaroline, delafloxacin, or linezolid added. The colony filter biofilms were allowed to grow for an additional 48 h, with transfer to a fresh plate containing the same antibiotic growth conditions after 24 h. After 48 h of antibiotic exposure, the filters containing the biofilms were transferred to a microcentrifuge tube and frozen at −20 °C until protein extraction could be performed. In each experiment, three colony biofilm filters were pooled for each sample, and the experiment was repeated in triplicate. Protein extraction was performed by washing the filters in SA lysis solution (50 mM TrisHCl pH7.5, 20 mM $MgCl_2$, Roche Complete protease inhibitors) and vortexing to separate the biofilm from the filters and resuspend the bacteria. The samples were washed once with SA lysis solution, and then resuspended in SA lysis solution with 40 μg/ml of lysostaphin (AMBI Products) and incubated at 37 °C for 1 h. Following lysostaphin digestion, IGEPAL (Sigma Aldrich) was added to a final concentration of 1% and the samples were incubated on ice for 15 minutes prior to sonication. Following sonication, the cellular debris was pelleted by centrifugation, and the supernatant was transferred to a fresh microcentrifuge tube and stored at −20 °C prior to LC-MS/MS analysis.

### LC-MS/MS

To generate quantitative proteomics data, proteins were solubilized with 5% SDS, 50 mM TEAB (pH 7.6), incubated at 95 °C for 5 min, and sonicated at 20% amplitude. Protein concentrations were determined using the Pierce 660 Assay (Thermo Scientific), and equal amounts of protein were digested using S-traps (Protifi). Briefly, proteins were reduced with dithiothreitol (DTT), alkylated with iodoacetamide (IAA), acidified using phosphoric acid, and combined with s-trap loading buffer (90% MeOH, 100 mM TEAB). Proteins were loaded onto s-traps, washed, and digested with Trypsin/Lys-C overnight at 37 °C. Peptides were eluted and dried with a vacuum concentrator. Peptides were resuspended in H2O/0.1% formic acid for LC-MS/MS analysis.

Peptides were separated using a 75 μm x 50 cm C18 reversed-phase-HPLC column (Thermo Scientific) on an Ultimate 3000 UHPLC (Thermo Scientific) with a 120 min gradient (2–32% ACN with 0.1% formic acid) and analyzed on a hybrid quadrupole-Orbitrap instrument (Q Exactive Plus, Thermo Fisher Scientific). Full MS survey scans were acquired at 70,000 resolution. The top 10 most abundant ions were selected for MS/MS analysis.

### Proteome bioinformatic analysis

Raw data files were processed in MaxQuant v2.0.1.0 (www.maxquant.org)[82] and searched against the current Uniprot *S. aureus* protein sequences database. Search parameters include constant modification of cysteine by carbamidomethylation and the variable modification, methionine oxidation. Proteins are identified using the filtering criteria of 1% protein and peptide false discovery rate. Raw LFQ intensity data were log 2 transformed and analyzed using Perseus v1.6.15.0 (www.maxquant.org)[83]. P-values were calculated using a two-sided Welch's t-test and adjusted for multiple comparisons using a Permutation-based False Discovery Rate (FDR) method with an FDR cutoff of 0.05.

### Transposon library construction

A transposon library was constructed in the JE2 strain using the plasmids pBursa and pMG020 as described in ref. 30. The library construction process was repeated multiple times until enough transposon mutants could be pooled together to make a single library. This pooled library was grown for an additional 4 h in TSB (without antibiotics) before being frozen in individual aliquots at a concentration of roughly $1 \times 10^{11}$ CFUs/ml at −80 °C. Spot plating of the inoculum on TSA plates containing antibiotics (either 10 μg/ml tetracycline or 10 μg/ml chloramphenicol) confirmed curing of plasmids pBursa and pMG020 in greater than 99.98% of bacterial cells. The library was confirmed to have roughly 150,000 independent transposon mutants as verified by Illumina sequencing analysis. Pooled aliquots of this high-density library were frozen at −80 °C until used.

### Transposon library screen

A single aliquot of the frozen JE2 transposon library was thawed on ice, diluted 1:100 in PBS, and 10 μL (corresponding to ~$1 \times 10^7$ CFUs) of the diluted transposon library were inoculated on a polycarbonate filter to form a colony filter biofilm as above. These biofilms were grown on TSA for 48 h prior to being transferred to TSA plates either without antibiotics or with vancomycin, ceftaroline, delafloxacin, or linezolid added. The biofilms were grown for an additional 48 h, as above. After 48 h of antibiotic exposure, the filters containing the biofilms were transferred to a microcentrifuge tube, washed with 1 mL PBS, and vortexed to separate the biofilm from the filters and resuspend the bacteria. The resulting suspension was then diluted 1:500 into fresh TSB without antibiotics and outgrown for 4 h to enrich for viable bacteria. In addition to collecting samples after 48 h of antibiotic exposure, samples were also collected prior to transfer to antibiotic containing media, to serve as a $T_0$ comparison. The resulting culture was centrifuged, and the bacterial pellet was stored at −80 °C until DNA extraction could be performed. In each experiment, three colony biofilm filters were pooled for each sample, and the experiment was repeated in triplicate.

### Transposon sequencing analysis

The frozen bacteria pellets from the transposon library screen were thawed on ice and genomic DNA was extracted using the DNeasy Blood and Tissue Kit (Qiagen). Genomic DNA was sheared to 350 bp by sonication using a Covaris LE220 and prepared by sequencing using the homopolymer tail-mediated ligation PCR (HTML-PCR) as outlined in van Opijnen et al. [84]. with the modification of the use of the KAPA HiFi HotStart DNA Polymerase (Roche) for the PCR cycles and the use of the transposon-specific primers olj510 and olj511 as previously outlined[30]. Replicates were all individually barcoded and then multiplexed for sequencing. Sequencing was performed using a custom sequencing primer (olj512) on the HiSeq 2500 (Illumina) by the Tufts University Genomics Core Facility. Sequencing data were analyzed using the TRANSIT software package for TnSeq analysis (v3.2.7)[31]. Reads were processed and mapped to the *S. aureus* FPR3757 genome using the TnSeq Pre-Processor (TPP) tool. Gene essentiality was determining using the Gumbel method in TRANSIT. $Log_2$ fold changes between antibiotic exposed biofilms and the no antibiotic controls were calculated using the Resampling method in TRANSIT with beta-geometric normalization and correction for multiple comparisons using the Benjamini-Hochberg procedure.

### Homogenized biofilm assay

For assays involving mechanical disruption of biofilms, colony filter biofilms were grown for 48 h as described above. At that time, the filters containing the biofilms were transferred to 1.5 mL Red

Eppendorf Bead Lysis Kits (Next Advance, Inc) with 1 mL PBS and homogenizing using a Bullet Blender Tissue Homogenizer (Next Advance, Inc) run for 3 successive cycles at max speed at 4 °C. The biofilm homogenate, which did not include the filter, was transferred to a fresh microcentrifuge tube and centrifuged to pellet the bacteria., the resulting supernatant was discarded, and the bacteria were resuspended and diluted in CDM lacking arginine and other amino acids as appropriate for a given experiment at a ratio of 2.5 mL media per filter biofilm. The homogenized biofilm culture was then split into equal aliquots to which either a vehicle control or the missing amino acids were added to the appropriate concentration. The samples were then aliquoted into a 96 well plate and antibiotics were added individual wells, as appropriate for a given experiment. The plates were incubated at 37 °C with shaking at 180 rpm for up to 48 h. In addition to plating the homogenized cultures at the time of transfer to the 96 well plate, aliquots were also removed at 24 h and 48 hours, and serial dilutions were plated to determine CFUs remaining. Each experiment was repeated in triplicate with technical replicates used each time. Data were analyzed using either Student T-test or 2-way ANOVA depending on the number of conditions being tested, with the appropriate corrections for multiple comparisons included.

### Amino acid quantification

Colony filter biofilms grown for 48 h, as above, were weighed and stored at −80 °C. Amino acid extraction was performed by washing the filters in SA lysis solution and vortexing to separate the biofilm from the filters and resuspend the bacteria. The samples were washed once with SA lysis solution, and then resuspended in SA lysis solution with 40 μg/ml of lysostaphin (AMBI Products) and incubated at 37 °C for 1 h. Following lysostaphin digestion, 5-sulfosalicylic acid (Fisher Chemical) was added to a concentration of 20%, and the samples were sonicated. Following sonication, the cellular debris was pelleted by centrifugation, and the supernatant was transferred to a fresh microcentrifuge tube and stored at −20 °C prior to amino acid analysis. Amino acid concentrations were determined by HPLC by the VUMC Hormone Assay and Analytical Services Core using a dedicated Biochrom 30 amino acid analyzer.

### Labeling of nascent protein

Mature colony filter biofilms were homogenized as described above but were diluted into CDM lacking both arginine and methionine. The methionine analog L-homopropargylglycine (Thermo Fisher Scientific) was added to a final concentration of 470 μM and the culture was split into three equal aliquots to which either a vehicle control, L-arginine, or L-citrulline was added to a final concentration of 400 μM. These aliquots were split further, and a vehicle control or linezolid was added to a concentration of 20 μg/ml. The resulting cultures were incubated at 37 °C with shaking at 180 rpm. At 1 and 4 h following the split of the cultures, samples were collected from each culture. Cells were pelleted by centrifugation and stored at −80 °C for future use. The cell pellets were thawed on ice, washed once with SA lysis solution, and then resuspended in SA lysis solution with 40 μg/ml of lysostaphin (AMBI Products) and incubated at 37 °C for 15 min. Following lysostaphin digestion, SDS (Fisher Chemical) was added to a final concentration of 1% and the samples were incubated on ice for 15 min prior to sonication. Following sonication, the cellular debris was pelleted by centrifugation, and the supernatant was transferred to a fresh microcentrifuge tube and stored at −20 °C. Protein concentration in each sample was determined using a Pierce BCA Protein Assay Kit (Thermo Scientific) with SA lysis buffer containing lysostaphin used to normalize the protein concentrations. Equal concentrations of protein for each sample were used for click chemistry labeling using the Click-iT Protein Reaction Buffer Kit (Thermo Fisher Scientific) and Biotin Azide (Thermo Fisher Scientific) according to the manufacturer's instructions. The resulting samples were resolubilized in Laemmli Sample Buffer and run on an SDS-PAGE gel prior to transfer to a nitrocellulose membrane. Total protein was stained using Ponceau S stain (Sigma Aldrich) according to the manufacturer's instructions and then subsequently destained. The membrane was then blocked using Intercept Blocking Buffer (Li-Cor) and stained using IRDye 680RD Streptavidin (Li-Cor). Images of total protein staining with Ponceau S and nascent protein staining with IRDye 680RD Streptavidin were both captured using a ChemiDoc Imaging System (Bio-Rad) with the manufacturer's preprogramed settings for Ponceau S and IRDye 680RD, respectively. The integrated density of each sample was determined using imageJ analysis.

### Measurement of extracellular arginine depletion

Mature colony filter biofilms were homogenized as described above and diluted into CDM without arginine. The homogenized biofilm culture was then split into equal aliquots to which either a vehicle control or vancomycin was added to a final concentration of 400 μg/ml. A 1 mL sample was removed from each aliquot and pelleted by centrifugation. 200 μL of the resulting supernatant was removed and stored at −20 °C. L-arginine was added to the remaining aliquots to a final concentration of 400 μM and a second 1 mL sample was removed from each aliquot and pelleted by centrifugation. Two hundred μL of the resulting supernatant was removed and stored at −20 °C. The remaining aliquots were incubated at 37 °C with shaking at 180 rpm. At 1, 3, 6, and 24 h, samples were collected from each culture and processed in the same manner as the initial time 0 samples. Arginine concentrations in the samples were quantified by the VUMC Mass Spectrometry Research Center using an approach for amino acid quantification similar to what has been previously reported in ref. 85. Briefly, samples were spiked with an internal standard (Arginine-$^{15}N_4$, Sigma Aldrich) prior to extraction with methanol and derivatization with dansyl chloride (Sigma Aldrich). The dansyl derivative of L-arginine was measured by single reaction monitoring detection of dansyl derivatives (arginine: m/z 408 → 170, CE 30; arginine-$^{15}N_4$ internal standard: *m/z* 412 → 170, CE 30) using a Thermo TSQ Quantum triple stage quadrupole mass spectrometer (Thermo, Waltham, MA) interface to a Waters Acquity UPLC system (Waters, Milford, MA).

### Biofilm imaging by confocal microscopy

Colony filter biofilms were inoculated with a *S. aureus* USA300 LAC strain (AH1263) with constitutive GFP expression[86] and grown on TSA to maturity, as above. After 48 hours of growth, the filter biofilms were removed and partially embedded upside-down in a CMC/gelatin mix as previously described in ref. 87. Prior to freezing at −80 °C, the partially embedded biofilms were stained by the application of 50 μL of either FilmTracer™ SYPRO® Ruby biofilm matrix stain, SYTOX™ Red Dead Cell Stain, or Wheat Germ Agglutinin (WGA) Alexa Fluor 633 conjugate (Invitrogen) diluted in 0.9% NaCl to appropriate working concentrations per the manufacturers' recommendations. Stains were applied directly to the filter surface of the upside-down biofilm, allowed to incubate at room temperature for 15 min, and then washed off by 200 μL of 0.9% NaCl followed by an incubation period of 5 minutes with an additional 200 μL of 0.9% NaCl. After this was step the rest of the biofilm was covered with CMC/gelatin mix and frozen on a dry ice-isopentane slurry before being stored at −80 °C. The frozen biofilms were cryosectioned at a 10 μm thickness and thaw-mounted onto Superfrost™ microscope slides (Fisher Scientific). The biofilm cross-sections were imaged on the Zeiss LSM 880 Confocal Laser Scanning Microscope using the 20X air objective (0.80 Plan-Apochromat, WD = 0.55 mm).

### Murine superficial skin infection and treatment model

All mice were housed at the VUMC Animal facility with temperature between 69 and 75 °F and humidity between 30 and 70%. A 12-hour light-dark cycle was maintained. Mice were housed in groups of five

with free access to autoclaved water and food. All experimental manipulations were performed in a biosafety level 2 laminar flow hood. A well-established murine model of a skin and soft tissue infection was employed as previously described in ref. 44. Briefly, 6–8 week old C57BL/6 mice (Jackson Laboratories) were anesthetized using isoflurane. Tensoplast® adhesive bandages were used to remove fur from a roughly 2 cm × 2 cm patch on the back of a mouse. Overnight cultures of JE2 and *argH*::Tn were separately subcultured into TSB and grown to mid log phase, at which point they were washed with PBS and combined in an OD600-matched ratio of 2:1 (JE2 to *argH*::Tn). This ratio was chosen, instead of a 1:1 ratio, as it allowed a greater dynamic range over which a relative survival benefit for the marked mutant strain could be assessed. A 5 μL droplet of this bacterial suspension was spread on the exposed skin of the anesthetized mice and allowed to dry before the mice recovered from anesthesia. At 48 h post infection, a subset of mice were humanely euthanized, and their lesions were excised to enumerate the number of CFUs present. Mice were then treated for 48 h with twice daily intraperitoneal injections of either a 30 mg/kg of vancomycin (administered as a 3 mg/ml solution of vancomycin in PBS) or an equivalent volume of PBS alone (vehicle control). After 48 hours of treatment, the remaining mice were humanely euthanized, and their lesions were excised for CFU enumeration. Each lesion was placed in a 1.5 mL Navy Eppendorf Bead Lysis Kits (Next Advance, Inc) with 1 mL PBS and homogenizing them using a Bullet Blender Tissue Homogenizer (Next Advance, Inc) run for 3 successive cycles of 5 min at max speed at 4 °C. Serial dilutions of the homogenates were plated in triplicate to determine CFUs. Samples were plated on TSA plates containing 10 μg/ml erythromycin to determine the number of CFUs of *argH*::Tn present and were plated on TSA plates containing 2 μg/ml ciprofloxacin to determine the total number of CFUs of *S. aureus* present. This concentration of ciprofloxacin was used as it was separately determined to inhibit the growth of other skin flora without affecting the growth of JE2 or *argH*::Tn. The number of CFUs of JE2 present in a sample was calculated by subtracting the number of CFUs of *argH*::Tn from the total number of CFUs present. Samples were also plated on TSA without any antibiotics as a control to examine the presence of normal skin flora. In the case of skin samples that were analyzed for total amino acid content, mice had their fur removed by tape-stripping, as above. Immediately following the tape-stripping, the mice were euthanized, and their lesions were excised and weighed. The skin lesions were then transferred to 1.5 mL Navy Eppendorf Bead Lysis Kits (Next Advance, Inc) and a volume of ice cold 10% 5-sulfosalicylic acid equal to 3 times the weight was added. The samples were homogenizing using a Bullet Blender Tissue Homogenizer (Next Advance, Inc) run for 3 successive cycles of 5 min at max speed at 4 °C. The supernatant was removed and centrifuged at 3000 × g for 15 min at 4 °C, and the resulting supernatant was transferred to a fresh tube and spun for a second time at 3000 × g for 15 min before being transferred to a fresh microcentrifuge tube and stored at −20 °C prior to amino acid analysis. Amino acid concentrations were determined by HPLC by the VUMC Hormone Assay and Analytical Services Core using a dedicated Biochrom 30 amino acid analyzer.

### Murine osteomyelitis and treatment model

A previously established murine model of osteomyelitis was employed as previously described in ref. 50. Briefly, osteomyelitis was induced in 6–8 week old C57BL/6 mice (Jackson Laboratories) by direct inoculation of murine femurs with ~$1 \times 10^6$ CFUs of a 2:1 (JE2 to *argH*::Tn) mixture of mid-log phase bacteria. Starting immediately at the time of infection, mice were treated for 7 days with twice daily subcutaneous injections of either 15 mg/kg vancomycin or a vehicle control. Seven days post-infection mice were euthanized, and the infected femurs were removed. Femurs were homogenized and processed as described for the wound lesions above in order to determine the ratio of CFUs of JE2 to *argH*::Tn in each femur.

### Statistics & reproducibility

Statistical analyses were performed using GraphPad Prism v 10.1.2 unless otherwise stated. 1-way or 2-way ANOVA with Tukey multiple comparisons test or a two-sided Wilcoxon Signed Rank Test were used as indicated in the figure legends. For the Supplementary Figs., two-sided Student T-test, 2-way ANOVA with either Tukey or Šídák multiple comparisons test, two-sided multiple T-test with Holm-Šídák multiple comparisons test, or a two-sided Wilcoxon Signed Rank Test were used as indicated in the figure legends. In most cases, unless otherwise stated, data presented are technical replicates of biological triplicates. No statistical method was used to predetermine sample size. Instead, sample size was selected based on prior experience to maximize the ability to find statistically significant and meaningful differences between groups when experiments were replicated multiple times.

### Reporting summary

Further information on research design is available in the Nature Portfolio Reporting Summary linked to this article.

## Data availability

The data supporting the findings of this study are included in the manuscript, Supplementary, Supplementary Data files, or as part of the source data provided with this paper within the Source Data file. The TnSeq data generated in this study have been deposited in the National Center for Biotechnology Information (NCBI) Gene Expression Omnibus (GEO) under accession number: GSE267626. The mass spectrometry proteomics data generated in this study have been deposited to the ProteomeXchange Consortium via the PRIDE partner repository with the dataset identifier PXD052440. Source data are provided with this paper.

## References

1. Ikuta, K. S. et al. Global mortality associated with 33 bacterial pathogens in 2019: a systematic analysis for the Global Burden of Disease Study 2019. *Lancet* **400**, 2221–2248 (2022).
2. van der Vaart, T. W. et al. All-cause and infection-related mortality in *Staphylococcus aureus* bacteremia, a multicenter prospective cohort study. *Open Forum Infect. Dis.* **9**, ofac653 (2022).
3. Tong, S. Y. C., Davis, J. S., Eichenberger, E., Holland, T. L. & Fowler, V. G. *Staphylococcus aureus* infections: epidemiology, pathophysiology, clinical manifestations, and management. *Clin. Microbiol. Rev.* **28**, 603–661 (2015).
4. Chang, F.-Y. et al. A prospective multicenter study of *Staphylococcus aureus* bacteremia: incidence of endocarditis, risk factors for mortality, and clinical impact of methicillin resistance. *Med. (Baltim.)* **82**, 322–332 (2003).
5. Liao, C.-H., Chen, S.-Y., Huang, Y.-T. & Hsueh, P.-R. Outcome of patients with meticillin-resistant *Staphylococcus aureus* bacteraemia at an Emergency Department of a medical centre in Taiwan. *Int. J. Antimicrob. Agents* **32**, 326–332 (2008).
6. Khatib, R. et al. Persistence in *Staphylococcus aureus* bacteremia: incidence, characteristics of patients and outcome. *Scand. J. Infect. Dis.* **38**, 7–14 (2006).
7. Neuner, E. A., Casabar, E., Reichley, R. & McKinnon, P. S. Clinical, microbiologic, and genetic determinants of persistent methicillin-resistant *Staphylococcus aureus* bacteremia. *Diagn. Microbiol. Infect. Dis.* **67**, 228–233 (2010).
8. Hawkins, C. et al. Persistent *Staphylococcus aureus* bacteremia: an analysis of risk factors and outcomes. *Arch. Intern. Med.* **167**, 1861–1867 (2007).
9. Austin, E. D. et al. Reduced mortality of *Staphylococcus aureus* bacteremia in a retrospective cohort study of 2139 patients: 2007–2015. *Clin. Infect. Dis.* **70**, 1666–1674 (2020).
10. Shariati, A. et al. The global prevalence of Daptomycin, Tigecycline, Quinupristin/Dalfopristin, and Linezolid-resistant *Staphylococcus*

*aureus* and coagulase-negative staphylococci strains: a systematic review and meta-analysis. *Antimicrob. Resist. Infect. Control* **9**, 56 (2020).
11. Richter, S. S. et al. Activity of ceftaroline and epidemiologic trends in *Staphylococcus aureus* isolates collected from 43 medical centers in the United States in 2009. *Antimicrob. Agents Chemother.* **55**, 4154–4160 (2011).
12. Cai, Y. et al. The role of *Staphylococcus aureus* small colony variants in intraosseous invasion and colonization in periprosthetic joint infection. *Bone Jt. Res.* **11**, 843–853 (2022).
13. Gimza, B. D. & Cassat, J. E. Mechanisms of antibiotic failure during *Staphylococcus aureus* osteomyelitis. *Front. Immunol.* **12**, 638085 (2021).
14. Loss, G. et al. *Staphylococcus aureus* small colony variants (SCVs): news from a chronic prosthetic joint infection. *Front. Cell. Infect. Microbiol.* **9**, 363 (2019).
15. Meredith, E. M., Harven, L. T. & Berti, A. D. Antimicrobial efficacy against antibiotic-tolerant *Staphylococcus aureus* depends on the mechanism of antibiotic tolerance. *Antibiotics (Basel).* **11**, 1810 (2022).
16. Vasudevan, S. et al. Emergence of persister cells in *Staphylococcus aureus*: calculated or fortuitous move? *Crit. Rev. Microbiol*. 1–12 https://doi.org/10.1080/1040841X.2022.2159319. (2022).
17. Rowe, S. E., Beam, J. E. & Conlon, B. P. Recalcitrant *Staphylococcus aureus* infections: obstacles and solutions. *Infect. Immun.* **89**, e00694–20 (2021).
18. Kuehl, R., Morata, L., Meylan, S., Mensa, J. & Soriano, A. When antibiotics fail: a clinical and microbiological perspective on antibiotic tolerance and persistence of *Staphylococcus aureus*. *J. Antimicrob. Chemother.* **75**, 1071–1086 (2020).
19. Fauerharmel-Nunes, T. et al. MRSA isolates from patients with persistent bacteremia generate nonstable small colony variants in vitro within macrophages and endothelial cells during prolonged vancomycin exposure. *Infect. Immun.* **91**, e0042322 (2023).
20. Balaban, N. Q. et al. Definitions and guidelines for research on antibiotic persistence. *Nat. Rev. Microbiol.* **17**, 441–448 (2019).
21. Lewis, K. Riddle of biofilm resistance. *Antimicrob. Agents Chemother.* **45**, 999–1007 (2001).
22. Archer, N. K. et al. *Staphylococcus aureus* biofilms. *Virulence* **2**, 445–459 (2011).
23. Anderl, J. N., Franklin, M. J. & Stewart, P. S. Role of antibiotic penetration limitation in *Klebsiella pneumoniae* biofilm resistance to ampicillin and ciprofloxacin. *Antimicrob. Agents Chemother.* **44**, 1818–1824 (2000).
24. James, G. A. et al. Biofilms in chronic wounds. *Wound Repair Regen. Publ. Wound Heal. Soc. Eur. Tissue Repair Soc.* **16**, 37–44 (2008).
25. Wolcott, R. D. et al. Analysis of the chronic wound microbiota of 2,963 patients by 16S rDNA pyrosequencing. *Wound Repair Regen.* **24**, 163–174 (2016).
26. Gonzalez, T. et al. Biofilm propensity of *Staphylococcus aureus* skin isolates is associated with increased atopic dermatitis severity and barrier dysfunction in the MPAACH pediatric cohort. *Allergy* **76**, 302–313 (2021).
27. Zenelaj, B., Bouvet, C., Lipsky, B. A. & Uçkay, I. Do diabetic foot infections with methicillin-resistant *Staphylococcus aureus* differ from those with other pathogens? *Int. J. Low. Extrem. Wounds* **13**, 263–272 (2014).
28. Westgeest, A. C. et al. Global differences in the management of *Staphylococcus aureus* bacteremia: no international standard of care. *Clin. Infect. Dis.* **77**, 1092-1101 (2023).
29. Gilbert, D. N., Chambers, H. F., Eliopoulos, G. M., Saag, M. S. & Pavia, A. *Sanford Guide to Antimicrobial Therapy 2023*. (Antimicrobial Therapy, Sperryville, Va, 2023).
30. Grosser, M. R. et al. Genetic requirements for *Staphylococcus aureus* nitric oxide resistance and virulence. *PLoS Pathog.* **14**, e1006907 (2018).
31. DeJesus, M. A., Ambadipudi, C., Baker, R., Sassetti, C. & Ioerger, T. R. TRANSIT-A Software Tool for Himar1 TnSeq Analysis. *PLoS Comput. Biol.* **11**, e1004401 (2015).
32. Chaudhuri, R. R. et al. Comprehensive identification of essential *Staphylococcus aureus genes* using Transposon-Mediated Differential Hybridisation (TMDH). *BMC Genomics* **10**, 291 (2009).
33. Fey, P. D. et al. A genetic resource for rapid and comprehensive phenotype screening of nonessential *Staphylococcus aureus* genes. *mBio* **4**, e00537–00512 (2013).
34. Audretsch, C., Gratani, F., Wolz, C. & Dandekar, T. Modeling of stringent-response reflects nutrient stress induced growth impairment and essential amino acids in different *Staphylococcus aureus* mutants. *Sci. Rep.* **11**, 9651 (2021).
35. Nuxoll, A. S. et al. CcpA regulates arginine biosynthesis in *Staphylococcus aureus* through repression of proline catabolism. *PLoS Pathog.* **8**, e1003033 (2012).
36. Jeong, B. et al. *Staphylococcus aureus* does not synthesize arginine from proline under physiological conditions. *J. Bacteriol.* **204**, e0001822 (2022).
37. Reslane, I. et al. Catabolic ornithine carbamoyltransferase activity facilitates growth of *Staphylococcus aureus* in defined medium lacking glucose and arginine. *mBio* **13**, e0039522 (2022).
38. Reslane, I. et al. Glutamate-dependent arginine biosynthesis requires the inactivation of spoVG, sarA, and ahrC in *Staphylococcus aureus*. *J. Bacteriol.* **206**, e00337-23 (2024).
39. Gloag, E. S. et al. Arginine induced *Streptococcus gordonii* biofilm detachment using a novel rotating-disc rheometry method. *Front. Cell. Infect. Microbiol.* **11**, 784388 (2021).
40. Geiger, T. et al. The stringent response of *Staphylococcus aureus* and its impact on survival after phagocytosis through the induction of intracellular PSMs expression. *PLoS Pathog.* **8**, e1003016 (2012).
41. Salzer, A. & Wolz, C. Role of (p)ppGpp in antibiotic resistance, tolerance, persistence and survival in Firmicutes. *microLife* **4**, uqad009 (2023).
42. Gratani, F. L. et al. Regulation of the opposing (p)ppGpp synthetase and hydrolase activities in a bifunctional RelA/SpoT homologue from *Staphylococcus aureus*. *PLoS Genet* **14**, e1007514 (2018).
43. Debats, I. B. J. G. et al. Infected chronic wounds show different local and systemic arginine conversion compared with acute wounds. *J. Surg. Res.* **134**, 205–214 (2006).
44. Klopfenstein, N. et al. Murine models for staphylococcal infection. *Curr. Protoc.* **1**, e52 (2021).
45. Akiyama, H., Huh, W., Yamasaki, O., Oono, T. & Iwatsuki, K. Confocal laser scanning microscopic observation of glycocalyx production by *Staphylococcus aureus* in mouse skin: does *S. aureus* generally produce a biofilm on damaged skin? *Br. J. Dermatol.* **147**, 879–885 (2002).
46. Wanke, I. et al. *Staphylococcus aureus* skin colonization is promoted by barrier disruption and leads to local inflammation. *Exp. Dermatol.* **22**, 153–155 (2013).
47. Schierle, C. F., De la Garza, M., Mustoe, T. A. & Galiano, R. D. Staphylococcal biofilms impair wound healing by delaying reepithelialization in a murine cutaneous wound model. *Wound Repair Regen.* **17**, 354–359 (2009).
48. Kugelberg, E. et al. Establishment of a Superficial Skin Infection Model in Mice by Using *Staphylococcus aureus* and *Streptococcus pyogenes*. *Antimicrob. Agents Chemother.* **49**, 3435–3441 (2005).
49. Castleman, M. J. et al. Innate Sex Bias of *Staphylococcus aureus* Skin Infection Is Driven by α-Hemolysin. *J. Immunol. Baltim. Md 1950* **200**, 657–668 (2018).
50. Spoonmore, T. J., Ford, C. A., Curry, J. M., Guelcher, S. A. & Cassat, J. E. Concurrent Local Delivery of Diflunisal Limits Bone Destruction but Fails To Improve Systemic Vancomycin Efficacy during *Staphylococcus aureus* Osteomyelitis. *Antimicrob. Agents Chemother.* **64**, e00182–20 (2020).

51. Gardete, S., Wu, S. W., Gill, S. & Tomasz, A. Role of VraSR in antibiotic resistance and antibiotic-induced stress response in *Staphylococcus aureus*. *Antimicrob. Agents Chemother.* **50**, 3424–3434 (2006).
52. Machado, H. et al. Environmental conditions dictate differential evolution of vancomycin resistance in *Staphylococcus aureus*. *Commun. Biol.* **4**, 793 (2021).
53. Fernandes, P. B., Reed, P., Monteiro, J. M. & Pinho, M. G. Revisiting the role of VraTSR in *Staphylococcus aureus* response to cell wall-targeting antibiotics. *J. Bacteriol.* **204**, e0016222 (2022).
54. Sun, H., Yang, Y., Xue, T. & Sun, B. Modulation of cell wall synthesis and susceptibility to vancomycin by the two-component system AirSR in *Staphylococcus aureus* NCTC8325. *BMC Microbiol.* **13**, 286 (2013).
55. Chen, L. et al. The role of *graRS* in regulating virulence and antimicrobial resistance in methicillin-resistant *Staphylococcus aureus*. *Front. Microbiol.* **12**, 727104 (2021).
56. Trotonda, M. P., Xiong, Y. Q., Memmi, G., Bayer, A. S. & Cheung, A. L. Role of *mgrA* and *sarA* in methicillin-resistant *Staphylococcus aureus* autolysis and resistance to cell wall-active antibiotics. *J. Infect. Dis.* **199**, 209–218 (2009).
57. Rajagopal, M. et al. Multidrug intrinsic resistance factors in *Staphylococcus aureus* identified by profiling fitness within high-diversity transposon libraries. *mBio* **7**, e00950–16 (2016).
58. Kuroda, M. et al. Two-component system VraSR positively /modulates the regulation of cell-wall biosynthesis pathway in *Staphylococcus aureus*. *Mol. Microbiol.* **49**, 807–821 (2003).
59. Caldelari, I., Loeliger, B., Langen, H., Glauser, M. P. & Moreillon, P. Deregulation of the arginine deiminase (*arc*) operon in penicillin-tolerant mutants of *Streptococcus gordonii*. *Antimicrob. Agents Chemother.* **44**, 2802–2810 (2000).
60. Freiberg, J. A. et al. The arginine deiminase pathway impacts antibiotic tolerance during biofilm-mediated *Streptococcus pyogenes* infections. *mBio* **11**, e00919–e00920 (2020).
61. Borriello, G., Richards, L., Ehrlich, G. D. & Stewart, P. S. Arginine or nitrate enhances antibiotic susceptibility of *Pseudomonas aeruginosa* in biofilms. *Antimicrob. Agents Chemother.* **50**, 382–384 (2006).
62. Ladjouzi, R. et al. Loss of antibiotic tolerance in Sod-deficient mutants Is dependent on the energy source and arginine catabolism in *Enterococci*. *J. Bacteriol.* **197**, 3283–3293 (2015).
63. Schrader, S. M. et al. Multiform antimicrobial resistance from a metabolic mutation. *Sci. Adv.* **7**, eabh2037 (2021).
64. Ocampo, P. S. et al. Antagonism between Bacteriostatic and Bactericidal Antibiotics Is Prevalent. *Antimicrob. Agents Chemother.* **58**, 4573–4582 (2014).
65. Conlon, B. P. et al. Persister formation in *Staphylococcus aureus* is associated with ATP depletion. *Nat. Microbiol.* **1**, 16051 (2016).
66. Rowe, S. E. et al. Reactive oxygen species induce antibiotic tolerance during systemic *Staphylococcus aureus* infection. *Nat. Microbiol.* **5**, 282–290 (2020).
67. Beam, J. E. et al. Macrophage-produced peroxynitrite induces antibiotic tolerance and supersedes intrinsic mechanisms of persister formation. *Infect. Immun.* **89**, e0028621 (2021).
68. Geiger, T., Kästle, B., Gratani, F. L., Goerke, C. & Wolz, C. Two small (p)ppGpp synthases in *Staphylococcus aureus* mediate tolerance against cell envelope stress conditions. *J. Bacteriol.* **196**, 894–902 (2014).
69. Cunin, R., Glansdorff, N., Piérard, A. & Stalon, V. Biosynthesis and metabolism of arginine in bacteria. *Microbiol. Rev.* **50**, 314–352 (1986).
70. Iyengar, R., Stuehr, D. J. & Marletta, M. A. Macrophage synthesis of nitrite, nitrate, and N-nitrosamines: precursors and role of the respiratory burst. *Proc. Natl Acad. Sci.* **84**, 6369–6373 (1987).
71. Halsey, C. R. et al. Amino acid catabolism in *Staphylococcus aureus* and the function of carbon catabolite repression. *mBio* **8**, e01434–16 (2017).
72. Manna, A. C. et al. Teg58, a small regulatory RNA, is involved in regulating arginine biosynthesis and biofilm formation in *Staphylococcus aureus*. *Sci. Rep.* **12**, 14963 (2022).
73. Abdelhady, W. et al. Impact of vancomycin on sarA-mediated biofilm formation: role in persistent endovascular infections due to methicillin-resistant *Staphylococcus aureus*. *J. Infect. Dis.* **209**, 1231–1240 (2014).
74. Diekema, D. J. et al. Continued emergence of USA300 methicillin-resistant *Staphylococcus aureus* in the United States: results from a nationwide surveillance study. *Infect. Control Hosp. Epidemiol.* **35**, 285–292 (2014).
75. Diep, B. A. et al. Complete genome sequence of USA300, an epidemic clone of community-acquired meticillin-resistant *Staphylococcus aureus*. *Lancet* **367**, 731–739 (2006).
76. Thurlow, L. R. et al. Functional modularity of the arginine catabolic mobile element contributes to the success of USA300 methicillin-resistant *Staphylococcus aureus*. *Cell Host Microbe* **13**, 100–107 (2013).
77. Davis, J. S. & Anstey, N. M. Is plasma arginine concentration decreased in patients with sepsis? A systematic review and meta-analysis. *Crit. Care Med.* **39**, 380–385 (2011).
78. Wijnands, K. A. P., Castermans, T. M. R., Hommen, M. P. J., Meesters, D. M. & Poeze, M. Arginine and citrulline and the immune response in sepsis. *Nutrients* **7**, 1426–1463 (2015).
79. Duthie, E. S. & Lorenz, L. L. Staphylococcal coagulase; mode of action and antigenicity. *J. Gen. Microbiol.* **6**, 95–107 (1952).
80. Chen, J., Yoong, P., Ram, G., Torres, V. J. & Novick, R. P. Single-copy vectors for integration at the SaPI1 attachment site for *Staphylococcus aureus*. *Plasmid* **76**, 1–7 (2014).
81. Vitko, N. P. & Richardson, A. R. Laboratory maintenance of methicillin-resistant *Staphylococcus aureus* (MRSA). *Curr. Protoc. Microbiol.* **Chapter 9**, Unit 9C.2 (2013).
82. Cox, J. & Mann, M. MaxQuant enables high peptide identification rates, individualized p.p.b.-range mass accuracies and proteome-wide protein quantification. *Nat. Biotechnol.* **26**, 1367–1372 (2008).
83. Tyanova, S. et al. The Perseus computational platform for comprehensive analysis of (prote)omics data. *Nat. Methods* **13**, 731–740 (2016).
84. van Opijnen, T., Lazinski, D. W. & Camilli, A. Genome-wide fitness and genetic interactions determined by tn-seq, a high-throughput massively parallel sequencing method for microorganisms. *Curr. Protoc. Microbiol.* **36**, 1E.3.1–1E.3.24 (2015).
85. Desine, S. et al. Association of alpha-aminoadipic acid with cardiometabolic risk factors in healthy and high-risk individuals. *Front. Endocrinol.* **14**, 1122391 (2023).
86. Ryan, D. J. et al. MicroLESA: Integrating Autofluorescence Microscopy, In Situ Micro-Digestions, and Liquid Extraction Surface Analysis for High Spatial Resolution Targeted Proteomic Studies. *Anal. Chem.* **91**, 7578–7585 (2019).
87. Rivera, E. S. et al. Imaging mass spectrometry reveals complex lipid distributions across *Staphylococcus aureus* biofilm layers. *J. Mass Spectrom. Adv. Clin. Lab.* **26**, 36–46 (2022).


## Acknowledgements

Plasmids pBursa and pMG020 used in the construction of a transposon library were graciously provided by Dr. Anthony Richardson. We appreciate the assistance of Dr. Dale Chaput and the University of South Florida Proteomics & Mass Spectrometry Core Facility for assistance with the proteomics experiments. We appreciate the assistance of the VUMC Analytical Services Core (supported by NIH grants DK059637 and DK020593) with the amino acid quantification experiments. We

appreciate the Tufts University Core Facility Genomics Core for assistance with the transposon sequencing experiments. Confocal microscopy was performed in part through the use of the Vanderbilt Cell Imaging Shared Resource (supported by NIH grants CA68485, DK20593, DK58404, DK59637, EY08126, and S10OD021630). J.A.F. received support from the VUMC Faculty Research Scholars program along with support from the National Institutes of Health (NIH) through an F32 postdoctoral fellowship (AI169905). J.A.F. and B.D.G. received support from the National Institutes of Health (NIH) through a T32 training grant (AI007540). V.M.R.R. was supported by the Howard Hughes Medical Institute as an HHMI Hanna Gray Fellow and by the Academic Pathways program from Vanderbilt University. V.M.R.R. holds a Postdoctoral Enrichment Program Award from the Burroughs Wellcome Fund. C.C.M. was supported by K99GM151477. J.E.C. was supported by R01AI145992, R01AI161022, R01AI173795, and the Mathers Foundation. This work was funded by R01AI150701, R01AI138581, R01AI17829, and R01AI145992 to E.P.S. We appreciate members of the Skaar laboratory for providing critical review and feedback of this manuscript.

## Author contributions

J.A.F. and E.P.S. designed research, analyzed data, and wrote the paper; J.A.F., B.D.G., C.C.M., J.M.C., and J.E.C. performed the research; J.A.F., V.M.R.R., and E.R.G. contributed new reagents or analytic tools.

## Competing interests

The authors declare no competing interests.

## Additional information

**Supplementary information** The online version contains supplementary material available at https://doi.org/10.1038/s41467-024-51144-9.

**Correspondence** and requests for materials should be addressed to Jeffrey A. Freiberg or Eric P. Skaar.

**Peer review information** *Nature Communications* thanks Vinai Thomas, and the other, anonymous, reviewer(s) for their contribution to the peer review of this work. A peer review file is available.